bioRxiv preprint doi: https://doi.org/10.1101/2021.11.03.467116; this version posted November 8, 2021. The copyright holder for this preprint (which was not certified by peer review) is the author/funder. All rights reserved. No reuse allowed without permission.

Detection of the HIV-1 accessory proteins Nef and Vpu by flow cytometry represents a new tool to study their functional interplay within a single infected CD4+ T cell

Jérémie Prévost[1,2,*], Jonathan Richard[1,2,*], Romain Gasser[1,2], Halima Medjahed[1], Frank Kirchhoff[3], Beatrice H. Hahn[4], John C. Kappes[5], Christina Ochsenbauer[5], Ralf Duerr[6], Andrés Finzi[1,2,7,#]

[1]Centre de Recherche du CHUM, Montreal, Quebec, Canada
[2]Département de Microbiologie, Infectiologie et Immunologie, Université de Montréal, Montreal, Quebec, Canada
[3]Institute of Molecular Virology, Ulm University Medical Center, Ulm, Germany.
[4]Departments of Medicine and Microbiology, Perelman School of Medicine, University of Pennsylvania, Philadelphia, PA, USA
[5]Department of Medicine, University of Alabama at Birmingham, Birmingham, AL, USA
[6]Department of Microbiology, New York University School of Medicine, New York, NY, USA
[7]Department of Microbiology and Immunology, McGill University, Montreal, Quebec, Canada

*Contributed equally

[#]**Corresponding author:**
Andrés Finzi
Centre de recherche du CHUM (CRCHUM)
900 St-Denis street, Tour Viger, R09.420
Montréal, Québec, H2X 0A9, Canada
andres.finzi@umontreal.ca
Phone: 514-890-8000 ext: 35264
Fax: 514-412-7936

Running Title: Nef and Vpu expression dictates ADCC responses

Key Words: HIV-1, Env, Nef, Vpu, CD4, BST-2, ADCC, LucR.T2A, non-neutralizing antibodies, CD4-bound conformation

bioRxiv preprint doi: https://doi.org/10.1101/2021.11.03.467116; this version posted November 8, 2021. The copyright holder for this preprint (which was not certified by peer review) is the author/funder. All rights reserved. No reuse allowed without permission.

ABSTRACT

The HIV-1 Nef and Vpu accessory proteins are known to protect infected cells from antibody-dependent cellular cytotoxicity (ADCC) responses by limiting exposure of CD4-induced (CD4i) envelope (Env) epitopes at the cell surface. Although both proteins target the host receptor CD4 for degradation, the extent of their functional redundancy is unknown. Here, we developed an intracellular staining technique that permits the intracellular detection of both Nef and Vpu in primary CD4+ T cells by flow cytometry. Using this method, we show that the combined expression of Nef and Vpu predicts the susceptibility of HIV-1-infected primary CD4+ T cells to ADCC by HIV+ plasma. We also show that Vpu cannot compensate for the absence of Nef, thus providing an explanation for why some infectious molecular clones that carry a LucR reporter gene upstream of Nef render infected cells more susceptible to ADCC responses. Our method thus represents a new tool to dissect the biological activity of Nef and Vpu in the context of other host and viral proteins within single infected CD4+ T cells.

IMPORTANCE

HIV-1 Nef and Vpu exert several biological functions that are important for viral immune evasion, release and replication. Here, we developed a new method allowing simultaneous detection of these accessory proteins in their native form together with some of their cellular substrates. This allowed us to show that Vpu cannot compensate the lack of a functional Nef, which has implication for studies that use Nef-defective viruses to study ADCC responses.

bioRxiv preprint doi: https://doi.org/10.1101/2021.11.03.467116; this version posted November 8, 2021. The copyright holder for this preprint (which was not certified by peer review) is the author/funder. All rights reserved. No reuse allowed without permission.

INTRODUCTION

The human immunodeficiency virus type 1 (HIV-1) genome encodes four accessory proteins (Vif, Vpr, Vpu and Nef), which are dispensable for viral replication *in vitro* but required for efficient replication, restriction factors counteraction and immune evasion *in vivo* (1-7). Among them, Nef and Vpu are well known for their role in subverting the host cell protein trafficking machinery (8, 9).

HIV-1 Nef is a small cytoplasmic protein of 27 kDa produced from early viral transcripts (10), which requires a myristoyl group on its N-terminus to traffic to intracellular and plasma membranes (11). Nef harbors a highly conserved dileucine motif in its C-terminal flexible loop that is responsible for the interaction with clathrin adaptors protein complexes (AP-1, AP-2 and AP-3) (12). Among these, interaction with AP-2 is required to downregulate the CD4 receptor from the surface of infected cells (13, 14) and target it for degradation in lysosomal compartments (15, 16).

HIV-1 Vpu is a small type-I transmembrane protein of 16 kDa produced late in the viral replication cycle (17, 18) and contains a short luminal N-terminal peptide followed by a single helical transmembrane domain and a C-terminal cytoplasmic domain (19-21). The cytoplasmic domain is comprised of two α-helices linked by a flexible loop known for its interaction with the $SCF^{\beta TRCP}$ E3 ubiquitin ligase complex via a conserved phosphoserine motif ($DS^{P}GNES^{P}$) (22, 23). Vpu mainly localizes within intracellular compartments, notably the endoplasmic reticulum (ER) and the *trans*-Golgi network (TGN) (24-26). Like Nef, Vpu also induces degradation of newly synthesized CD4 by directing it through an ER-associated pathway (ERAD) for further

bioRxiv preprint doi: https://doi.org/10.1101/2021.11.03.467116; this version posted November 8, 2021. The copyright holder for this preprint (which was not certified by peer review) is the author/funder. All rights reserved. No reuse allowed without permission.

proteasomal degradation (22, 27-29). In addition, Vpu sequesters the restriction factor BST-2 in the TGN using its transmembrane domain, thereby increasing the release of progeny virions (30-33).

CD4 downregulation by Nef and Vpu was previously reported to be critical for efficient viral replication in T cells by enhancing virion release and infectivity, and by preventing superinfection (34-39). CD4 downregulation is critical for immune evasion since the anti-Env antibody (Ab) response is dominated by non-neutralizing antibodies (nnAbs) that target Env in its "open" CD4-bound conformation (40-42). The interaction between CD4 and Env at the surface of HIV-1-infected cells has been shown to promote nnAbs binding to Env, leading to the elimination of infected cells through Fc-mediated effector functions, including antibody-dependant cellular cytotoxicity (ADCC) (41, 43). Nef and Vpu limit the presence of Env-CD4 complexes at the cell surface and thus protect infected cells against ADCC (41, 43, 44).

In previous studies, Nef and Vpu expression was mostly examined in transfected cell lines, frequently using tagged proteins (30, 31, 45, 46) or by performing Western blots and immunofluorescence microscopy in infected primary cells (47-52). However, both proteins are small, intracellularly located and present in low amounts, rendering their detection difficult. To facilitate their analysis in primary CD4+ T cells, we developed an intracellular staining technique to detect Nef and Vpu expression by flow cytometry, which allows the simultaneous detection of these proteins together with host and viral proteins within a single infected cell. Using this method, we show that Nef and Vpu expression predicts the susceptibility of HIV-1-infected primary CD4+ T cells to ADCC by HIV+ plasma. We also explain why decreased Nef

bioRxiv preprint doi: https://doi.org/10.1101/2021.11.03.467116; this version posted November 8, 2021. The copyright holder for this preprint (which was not certified by peer review) is the author/funder. All rights reserved. No reuse allowed without permission.

expression in widely-used reporter viruses increase the susceptibility of infected cells to ADCC responses.

RESULTS

Intracellular detection of Nef and Vpu in HIV-1-infected primary CD4+ T cells.

To facilitate detection of intracellular Nef, we obtained a polyclonal Nef antiserum through the NIH AIDS Reagent Program, which was generated by immunization of rabbits with a recombinant clade B Nef consensus protein produced in *E. coli* (53). In previous studies, this antibody detected native Nef proteins by Western blot and immunofluorescence microscopy in both transfected and infected cells (47, 54-56). Given the scarcity of anti-Vpu antibodies, we immunized rabbits with a peptide corresponding to the clade B Vpu C-terminal region (residues 69-81). A similar approach was previously used to generate a polyclonal antibody capable of detecting Vpu by Western blot and immunofluorescence microscopy (24, 57).

We first evaluated the ability of both Nef and Vpu antisera to recognize their cognate antigen using HEK 293T cells transfected with plasmids expressing the Nef or Vpu proteins from the transmitted/founder (T/F) virus CH058 (58, 59). Forty-eight hours post-transfection, cells were permeabilized and stained with the antisera, followed by detection with a fluorescently-labelled anti-rabbit secondary antibody. As expected, the Nef antiserum recognized only Nef transfected cells, while the Vpu antiserum recognized only Vpu transfected cells (Fig. 1A-C). To evaluate whether our method detected Nef and Vpu when expressed in a biologically relevant culture system, we infected primary CD4+ T cells with CH058 infectious molecular clones (IMC) encoding Nef, and/or Vpu proteins. While wildtype (WT)-infected cells were efficiently

bioRxiv preprint doi: https://doi.org/10.1101/2021.11.03.467116; this version posted November 8, 2021. The copyright holder for this preprint (which was not certified by peer review) is the author/funder. All rights reserved. No reuse allowed without permission.

recognized by both Nef and Vpu antisera, abrogation of Nef (Fig 1D-E) or Vpu (Fig. 1F-G) expression prevented the recognition of productively-infected cells as identified by Gag protein intracellular staining (p24+). Of note, mock-infected or uninfected bystander cells (p24-) where not detected by either antiserum, further confirming their specificity (Fig 1D-G).

We next examined the antiserum binding to Nef and Vpu proteins from different HIV-1 clades and groups as well as from closely related simian immunodeficiency viruses (SIV). Primary CD4+ T cells were infected with a panel of HIV-1 IMCs representing clades B, C, A1 and CRF01_AE. As expected, both Nef and Vpu antisera recognized their respective antigen in cells infected with clade B viruses since both were raised against clade B immunogens (Fig. 1H-I). The anti-Nef polyclonal antibody was also able to recognize Nef proteins from group M clades C, A1 and CRF01_AE as well as the Nef from a group O isolate. This recognition extended even to the Nef protein of a related SIVcpzPts strain (isolate TAN2) but not to chimeric simian-human immunodeficiency viruses (SHIV) which express a SIVmac Nef (Fig. 1H). The Vpu antiserum was less cross-reactive and failed to detect Vpu from clade C viruses (Fig. 1I). These findings confirmed the specificity and cross-reactivity of the intracellular detection of Nef and Vpu using infected primary CD4+ T cells.

Measuring CD4 and BST-2 downregulation in infected primary CD4+ T cells with or without Nef and Vpu expression.

The efficient detection of Nef and Vpu at the single cell level by flow cytometry allowed us to combine this approach with the quantification of CD4 and BST-2 expression levels on the cell surface. Productively-infected cells (p24+) expressing both Nef and Vpu had little detectable

bioRxiv preprint doi: https://doi.org/10.1101/2021.11.03.467116; this version posted November 8, 2021. The copyright holder for this preprint (which was not certified by peer review) is the author/funder. All rights reserved. No reuse allowed without permission.

CD4 and BST-2 compared to uninfected cells (Fig. 2A). In contrast, cells infected with Vpu or Nef mutant viruses differed in the extent of CD4 and BST-2 downregulation (Fig. 2A).

Vpu targets CD4 and BST-2 by different mechanisms. First, Vpu interacts with multiple transmembrane proteins, including BST-2, through its transmembrane domain (TMD), which sequesters these proteins in perinuclear compartments (32, 33, 60-63). Second, Vpu downregulates CD4 by interaction of its cytoplasmic domain with the cytoplasmic tail of CD4 (64-69). Consistent with these different interaction modes, Vpu-mediated CD4 and BST-2 degradation involves independent pathways (proteasomal and lysosomal degradation, respectively), both of which depend on polyubiquitination by the $SCF^{\beta TRCP}$ E3 ubiquitin ligase complex, recruited by Vpu using its highly conserved phosphoserine motif (22, 26, 70, 71). To examine whether we could measure the expression and activity of Vpu mutants by flow cytometry, we introduced mutations at critical residues of the Vpu TMD (A14L/A18L) or its phosphoserine motif (S52A/S56A). CH058 IMCs coding for wildtype or mutated Vpu proteins were used to infect primary CD4+ T cells. While the TMD mutations did not affect Vpu expression, the phosphoserine mutations led to a significant accumulation of intracellular Vpu proteins (Fig. 2B), most likely because Vpu is degraded together with its target protein as a ubiquitinated complex (24, 72, 73). Despite a higher expression, the Vpu phosphoserine mutant was unable to downregulate CD4 and marginally diminished in its capacity to antagonize BST-2 (Fig 2C-F). This is consistent with studies demonstrating that the recruitment of the $SCF^{\beta TRCP}$ E3 ubiquitin ligase complex and the degradation of BST-2 by Vpu is dissociable from its capacity to antagonize the restriction factor (32, 71, 74-76). In contrast, the Vpu TMD mutations did not affect Vpu's ability to target CD4 but completely abrogated its capacity to downregulate BST-2

bioRxiv preprint doi: https://doi.org/10.1101/2021.11.03.467116; this version posted November 8, 2021. The copyright holder for this preprint (which was not certified by peer review) is the author/funder. All rights reserved. No reuse allowed without permission.

(Fig 2C-F). Together, these results emphasize the need of measuring Nef and Vpu expression when studying their biological functions.

Nef and Vpu expression inversely correlates with ADCC responses.

CD4 downregulation by Nef and Vpu, together with Vpu-mediated BST-2 antagonism were found to be critical factors preventing the exposure of vulnerable CD4-induced Env epitopes, thus protecting HIV-1-infected cells from ADCC (41, 43, 44, 77-80). To investigate the link between Nef and Vpu expression and HIV-1-infected cells immune evasion, we infected activated primary CD4+ T cells from five HIV-negative individuals with two clade B IMCs, CH058 T/F and JR-FL, encoding functional or defective *nef* and *vpu* genes. Focusing on the productively-infected cells (p24+), we performed a comprehensive characterization of the patterns of viral protein expression including cell-surface Env (detected with the conformation-independent Ab 2G12), intracellular Nef and Vpu in combination with cell-surface levels of CD4 and BST-2. We also measured the specific recognition and elimination of infected cells by ADCC using the CD4-induced (CD4i) A32 monoclonal Ab (mAb). This antibody binds the cluster A region of the gp120 which is occluded in the "closed" trimer and therefore can only bind Env in the "open" CD4-bound conformation. We also tested 25 different plasma samples from chronically HIV-1-infected individuals. As expected, Nef was only expressed by WT and Vpu- constructs, while Vpu was only expressed by WT and Nef- constructs (Fig. 3A). Consistent with previous reports (43, 77, 78), deletion of Nef strongly impaired CD4 downregulation by both viruses but did not affect Env or BST-2 cell-surface levels. Vpu deletion mitigated CD4 downregulation to a lesser extent than Nef and abrogated BST-2 downmodulation, resulting in an overall increase in the amount of cell-surface Env (Fig. 3B). We noticed lower levels of the JR-

bioRxiv preprint doi: https://doi.org/10.1101/2021.11.03.467116; this version posted November 8, 2021. The copyright holder for this preprint (which was not certified by peer review) is the author/funder. All rights reserved. No reuse allowed without permission.

FL Vpu protein compared to CH058 Vpu, which was linked to a less effective Vpu-mediated CD4 downmodulation (Fig. 3B). The cumulative effect of Nef and Vpu on cell-surface levels of Env, CD4 and BST-2 prevented the recognition of infected cells and protected them from ADCC responses mediated by A32 and HIV+ plasma (Fig. 3C-D). In contrast, abrogation of Nef or Vpu expression resulted in increased recognition and susceptibility of infected cells to ADCC mediated by nnAbs (Fig. 3C-D). We performed correlation analyses to measure the level of association between the different cellular, virological and immunological variables (Fig 3E-F). We found that both Nef and Vpu established a large network of inverse correlations with cellular and immunological factors. Interestingly, Env levels hardly contributed to the network and were poorly associated with the immunological outcome, thus indicating that the overall amount of Env present at the surface does not dictate ADCC responses mediated by CD4i Abs or HIV+ plasma, but rather the conformation Env occupies. Apart from antibody binding, ADCC responses mediated by nnAbs correlated strongly with CD4 and Nef levels (Fig. 3E-F). Overall, Nef and Vpu expression inversely correlates with the susceptibility of HIV-1-infected cells to ADCC mediated by CD4i Abs and HIV+ plasma.

Impaired Nef expression from IMC LucR.T2A constructs enhance the susceptibility of infected cells to ADCC.

Infectious molecular clones encoding for the *Renilla* luciferase (LucR) reporter gene upstream of the *nef* sequence, and a T2A ribosome-skipping peptide to drive Nef expression are widely employed to quantify anti-HIV-1 ADCC responses (81-92). Despite evidence that Nef-mediated CD4 downregulation is impaired when using these IMCs (54, 79), a series of recent studies have hypothesized that Vpu can compensate for the absence of Nef expression and completely

bioRxiv preprint doi: https://doi.org/10.1101/2021.11.03.467116; this version posted November 8, 2021. The copyright holder for this preprint (which was not certified by peer review) is the author/funder. All rights reserved. No reuse allowed without permission.

downregulate CD4 on its own (93-97). To evaluate this hypothesis, we used our intracellular staining to measure Nef and Vpu expression levels and study their impact on ADCC responses mediated by nnAbs against cells infected with IMC-LucR.T2A constructs. Primary CD4+ T cells were infected with NL4.3-based IMCs that do (Env-IMC-LucR.T2A) or do not encode (Env-IMC) a LucR.T2A cassette. These IMCs express the Env ectodomain from two clade B viruses, CH058 T/F and YU-2. Consistent with the lack of Nef detection by Western blot (54, 79), insertion of the LucR.T2A cassette also impaired the detection of Nef by flow cytometry, while Vpu expression remained unchanged (Fig. 4A-B). However, we noted an accumulation of cell-surface CD4 for Env-IMC-LucR.T2A compared to *nef*-intact constructs (~20-fold higher) (Fig. 4C), which resulted in a significantly increased recognition and susceptibility of infected cells to ADCC responses mediated by A32 mAb and HIV+ plasma (Fig. 4D-E). Of note, both the binding and the ADCC responses mediated by nnAbs were strongly associated with CD4 levels and inversely correlated with Nef expression (Fig 4F-G). In contrast, these variables poorly correlated with Vpu expression. Based on these data, it seems clear that Vpu expression alone is not sufficient to prevent ADCC-mediated killing of infected cells and that HIV-1 requires both Nef and Vpu for efficient humoral response evasion.

Nef, Vpu and CD4 levels predict ADCC responses mediated by HIV+ plasma.

We next used univariate multiple linear regression (MLR) analysis to evaluate the capacity of different variables to predict ADCC responses mediated by HIV+ plasma. This model is based on the hypothesis that a linear relationship exists between the dependant variable quantified empirically and the independent variables that serve as predictive variables. In our model, the dependant variable is the ADCC responses mediated by plasma from HIV+ donors (ADCC

bioRxiv preprint doi: https://doi.org/10.1101/2021.11.03.467116; this version posted November 8, 2021. The copyright holder for this preprint (which was not certified by peer review) is the author/funder. All rights reserved. No reuse allowed without permission.

HIV+ plasma) and the independent variables are the cellular, virological and immunological factors measured on infected cells. To run the MLR model, we combined data obtained with the different viral constructs (Fig. 3 & 4) and plotted the mean ADCC obtained with 25 HIV+ plasma against a single virus on the X axis and the associated predicted ADCC value based on one or more independent variables on the Y axis. When looking at cellular factors, we noticed that only CD4 accurately predicts ADCC responses mediated by HIV+ plasma, independent of the viral strain (Fig. 5A). Even though BST-2 displayed a strong correlation with ADCC responses (Fig 3E), it was not predictive. When focusing on virological variables, we observed that Nef is the only significant ADCC predictive variable, albeit not as good as CD4 (Fig. 5A-B). However, combinations of Nef with Vpu or Env increased its predictive scores, reaching similar levels as CD4 when combined with Vpu (Fig. 5B). Of note, the strength of the prediction was not further improved when combining all three virological variables altogether. As for immunological variables, their capacity to predict ADCC by HIV+ plasma was found to be equivalent or even higher than for cellular and virological factors (Fig. 5C). Indeed, the binding of HIV+ plasma predicted ADCC values with a similar score as CD4 or Nef and Vpu combined, while the binding of A32 predicted ADCC by HIV+ plasma even better (Fig. 5A-C). This could be explained by the fact that A32-like Abs present in plasma from infected individuals are from the main class of Abs (anti-cluster A Abs) mediating ADCC responses against infected cells (41, 80, 81, 91, 98). In line with this interpretation, ADCC mediated by A32 was found to have a near-perfect predictive ability, suggesting that factors, other than antibody binding, are presumably needed to fully explain the ADCC phenotypes observed (Fig. 5C).

bioRxiv preprint doi: https://doi.org/10.1101/2021.11.03.467116; this version posted November 8, 2021. The copyright holder for this preprint (which was not certified by peer review) is the author/funder. All rights reserved. No reuse allowed without permission.

DISCUSSION

Unlike simple retroviruses, HIV-1 and related SIVs encode multiple accessory proteins that promote viral replication and immune evasion (99). Among them, Nef and Vpu modulate the expression, trafficking, localization and function of several host cell surface proteins, including the viral receptor CD4, restriction factors and homing receptors (28, 30, 31, 62, 69, 100-104). They also modulate a wide range of immunoreceptors to evade immune responses mediated by CD8+ T, NK and NKT cells (105-113) . Most of these host cell proteins are naturally expressed on primary CD4+ T cells, the preferential target of HIV-1. The detection of Nef and Vpu has previously been done in transfected cells (30, 31, 46, 48, 49, 114), which results in the overexpression of the viral proteins when compared to infected primary CD4+ T cells. Moreover, tagged viral proteins are frequently used to facilitate their detection (30, 31, 46, 48, 49, 114). Protein overexpression and/or tag insertion, have the potential to impact the trafficking and functions of these accessory proteins. To study Nef and Vpu's biological activities in a physiologically relevant system, we developed an intracellular staining method to detect native Nef and Vpu proteins in HIV-1-infected primary CD4+ T cells by flow cytometry. Using Nef and Vpu antisera, we detected both viral proteins with high specificity in cells productively infected (p24+) with multiple IMCs. The Nef antiserum was cross-reactive, detecting Nef from group M (clade B, C, A1 and CRF01_AE), from a group O isolate and from a closely related SIVcpz strain. In contrast, the Vpu antiserum recognized only clade B Vpu proteins, consistent with the fact that we used a peptide from the C-terminal region of clade B Vpu. This region is highly variable among group M viruses (115). More conserved regions of Vpu map to the transmembrane domain of the protein and the βTRCP binding site (116, 117). However, these regions are either buried into the plasma membrane or occluded by cellular partners, and thus are

bioRxiv preprint doi: https://doi.org/10.1101/2021.11.03.467116; this version posted November 8, 2021. The copyright holder for this preprint (which was not certified by peer review) is the author/funder. All rights reserved. No reuse allowed without permission.

not readily accessible for antibody recognition. While the generation of a broad Vpu antiserum is challenging, it may be possible to generate clade-specific Vpu antisera by immunization using peptides corresponding to the C-terminal region specific for a given clade.

Nef and Vpu intracellular detection by flow cytometry represents an excellent tool to study their biological activities in HIV-1-infected primary CD4+ T cells. This method allows for the detection of cell-surface substrates or antibody recognition of surface Env and the concomitant detection of Nef and Vpu expression within a single infected cell (Fig. 2A). Infected CD4+ T cells represent the most relevant system to study the complex interplay between these two accessory proteins and the wide range of host cell factors naturally expressed by T cells. Recent findings revealed that modulation of BST-2 levels by type I IFN impacts the capacity of Vpu to downregulate NTB-A, PVR, CD62L and Tim-3, thus reducing its polyfunctionality (63, 69). Nef and Vpu also display overlapping functions, as they share the capacity to downregulate several cell-surface proteins, including CD4, PVR, CD62L and CD28 (8, 56, 62, 110, 118). The expression levels of one viral protein could therefore modulate the biological activities of the other, making it essential to study their functions in a context where both viral proteins are expressed simultaneously at physiological levels. Thus, our intracellular staining measuring Nef/Vpu expression and functionality in HIV-1-infected cells represents a new approach to better characterize their functional interplay.

Increasing evidence points towards Env conformation on the surface of infected cells as a critical parameter of ADCC susceptibility to HIV+ plasma (41, 119-121). Non-neutralizing antibodies in the plasma from HIV-1-infected individuals target epitopes that are only exposed when Env

bioRxiv preprint doi: https://doi.org/10.1101/2021.11.03.467116; this version posted November 8, 2021. The copyright holder for this preprint (which was not certified by peer review) is the author/funder. All rights reserved. No reuse allowed without permission.

interacts with cell-surface CD4, thus adopting the "open" CD4-bound conformation (41, 43). Nef and Vpu contribute to protect HIV-1-infected cells from ADCC by limiting Env-CD4 interaction via CD4 downregulation and BST-2 antagonism (41, 43, 44, 77, 78). Here we confirm and extend previous observations by showing that Nef and Vpu expression predicts the susceptibility of HIV-1-infected primary CD4+ T cells to ADCC responses. In agreement with recent studies (44, 79), we found that CD4 accurately predicted the susceptibility of infected cells to ADCC (Fig. 5). Given its enhanced capacity to downregulate CD4 compared to Env or Vpu (34, 41, 43, 118), Nef represents the main viral factor influencing ADCC responses mediated by CD4-induced ligands (Fig. 5B). On the contrary, BST-2 and Env expression, alone or in combination, were unable to accurately predict the susceptibility of infected cells to ADCC. These results are consistent with previous reports suggesting that Env conformation rather than overall cell-surface Env levels, drives ADCC responses mediated by HIV+ plasma (41, 43, 120, 121). This is also in agreement with recent work showing that BST-2 upregulation by type I IFN enhances cell-surface Env levels without increasing the susceptibility of infected cells to ADCC mediated by HIV+ plasma, unless CD4-mimetics are used to "open-up" Env and stabilize the CD4-bound conformation (122).

A series of recent studies using LucR.T2A IMCs have hypothesized that Vpu can compensate for the absence of Nef expression by fully downregulating cell-surface CD4 (93-97). Our results show that this is not the case. Consistent with its role in targeting CD4 already present at the plasma membrane, the impact of Nef on CD4 downmodulation is more prominent (Fig. 2 & 3) (34, 41, 43, 118). In its absence, Vpu was unable to fully downregulate CD4, thus sensitizing infected cells to ADCC responses. These results highlight the importance of selecting full-length

bioRxiv preprint doi: https://doi.org/10.1101/2021.11.03.467116; this version posted November 8, 2021. The copyright holder for this preprint (which was not certified by peer review) is the author/funder. All rights reserved. No reuse allowed without permission.

unmutated IMCs with proper Nef and Vpu expression to generate biologically relevant ADCC measurements. For example, a recent manuscript recently reported no differences in ADCC susceptibility between cells infected with clade B, clade C or CRF01_AE IMCs (123) while previous studies have shown otherwise (120, 124). In this article (123), the authors use functionally Nef defective LucR.T2A IMCs, which results in incomplete CD4 downregulation and therefore exposure of Env in its CD4-bound conformation at the cell surface (Fig. 4) (79). Thus, it is not surprising that the usage of Nef defective viruses skew ADCC responses in favor of nnAbs and mitigate the intrinsic differences that exists between Env from different clades. Fortunately, several alternatives to the use of LucR.T2A IMCs are available to measure ADCC against productively-infected cells (125), including the Infected Cell Elimination (ICE) assay, which measures the loss of productively-infected cells (p24+) by flow cytometry and allows the utilization of unmodified IMCs. Utilization of an NK cells resistant T cell line expressing a Tat-driven luciferase reporter gene (CEM.NKr-CCR5-sLTR-Luc) as target cells also represents an option (126). Finally, luciferase reporter IMCs (referred to as LucR.6ATRi IMCs) expressing similar levels of Nef than those obtained with unmodified IMC are also available. These IMCs utilize a modified encephalomyocarditis virus (EMCV) internal ribosome entry site (IRES) element in lieu of T2A (54, 79). Thus, LucR.6ATRi reporter viruses represent a biologically relevant alternative to LucR.T2A IMCs when measuring ADCC mediated by nnAbs and plasma collected from infected or vaccinated individuals.

ACKNOWLEDGMENTS

The authors thank the CRCHUM BSL3 and Flow Cytometry Platforms for technical assistance, Mario Legault from the FRQS AIDS and Infectious Diseases network for cohort coordination

bioRxiv preprint doi: https://doi.org/10.1101/2021.11.03.467116; this version posted November 8, 2021. The copyright holder for this preprint (which was not certified by peer review) is the author/funder. All rights reserved. No reuse allowed without permission.

and clinical samples. We thank the following collaborators for kindly providing some infectious molecular clones: Dennis Burton (The Scripps Research Institute) for JR-FL, Malcom A. Martin (NIAID) for $SHIV_{AD8-EO}$, George M. Shaw (UPenn) for SHIV.AE.40100 and Sodsai Tovanabutra (US MHRP) for the $HIV\text{-}1_{WR27}$, $HIV\text{-}1_{703357}$, $HIV\text{-}1_{40061}$, $HIV\text{-}1_{CM235}$ and $HIV\text{-}1_{851891}$ IMCs. We thank MédiMabs for their scientific and technical support during the development of the Vpu antiserum. This study was supported by grants from the National Institutes of Health to A.F., C.O. and J.C.K. (R01 AI148379), to A.F. (R01 AI129769 and R01 AI150322) and to BHH (R01 AI162646 and UM1 AI164570). This work was also partially supported by 1UM1AI164562-01, co-funded by National Heart, Lung and Blood Institute, National Institute of Diabetes and Digestive and Kidney Diseases, National Institute of Neurological Disorders and Stroke, National Institute on Drug Abuse and the National Institute of Allergy and Infectious Diseases, a CIHR foundation grant #352417, a CIHR Team grant #422148 and a Canada Foundation for Innovation grant #41027 to A.F. A.F. is the recipient of a Canada Research Chair on Retroviral Entry #RCHS0235 950-232424. F.K. is supported by the Deutsche Forschungsgemeinschaft (CRC 1279 and SPP 1923). J.P. is the recipient of a CIHR doctoral fellowship. The funders had no role in study design, data collection and analysis, decision to publish, or preparation of the manuscript.

AUTHOR CONTRIBUTIONS

J.P. J.R. and A.F. conceived the study. J.P., J.R., and A.F. designed experimental approaches. J.P., J.R., R.G. R.D. and A.F. performed, analyzed, and interpreted the experiments. H.M., F.K., B.H.H., J.C.K. and C.O. supplied novel/unique reagents. J.P., J.R., BHH, and A.F. wrote the paper. All authors have read, edited, and approved the final manuscript.

bioRxiv preprint doi: https://doi.org/10.1101/2021.11.03.467116; this version posted November 8, 2021. The copyright holder for this preprint (which was not certified by peer review) is the author/funder. All rights reserved. No reuse allowed without permission.

CONFLICT OF INTEREST

The authors declare no competing interests.

DATA AVAILABILITY

Data and reagents are available upon request.

METHODS

Ethics Statement

Written informed consent was obtained from all study participants [the Montreal Primary HIV Infection Cohort (127, 128) and the Canadian Cohort of HIV Infected Slow Progressors (129-131), and research adhered to the ethical guidelines of CRCHUM and was reviewed and approved by the CRCHUM institutional review board (ethics committee, approval number CE 16.164 - CA). Research adhered to the standards indicated by the Declaration of Helsinki. All participants were adult and provided informed written consent prior to enrolment in accordance with Institutional Review Board approval.

Cell lines and isolation of primary cells

HEK293T human embryonic kidney cells (obtained from ATCC) were grown as previously described (132). Primary human PBMCs and CD4+ T cells were isolated, activated and cultured as previously described (43). Briefly, PBMCs were obtained by leukapheresis from HIV-

bioRxiv preprint doi: https://doi.org/10.1101/2021.11.03.467116; this version posted November 8, 2021. The copyright holder for this preprint (which was not certified by peer review) is the author/funder. All rights reserved. No reuse allowed without permission.

402 negative individuals (4 males and 1 female) and CD4+ T lymphocytes were purified from resting
403 PBMCs by negative selection using immunomagnetic beads per the manufacturer's instructions
404 (StemCell Technologies, Vancouver, BC) and were activated with phytohemagglutinin-L (10
405 µg/mL) for 48 hours and then maintained in RPMI 1640 complete medium supplemented with
406 rIL-2 (100 U/mL).
407
408 **Plasmids and proviral constructs**
409 The vesicular stomatitis virus G (VSV-G)-encoding plasmid was previously described (133).
410 Transmitted/Founder (T/F) and chronic infectious molecular clones (IMCs) of patients CH040,
411 CH058, CH077, CH131, CH141, CH167, CH185, CH198, CH236, CH269, CH293, CH440,
412 CH470, CH505, CH534, CH850, CM235, MCST, REJO, RHGA, RHPA, STCO, SUMA, TRJO,
413 WARO, WITO, WR27, 40061, 703357 and 851891 were inferred, constructed, and biologically
414 characterized as previously described (120, 134-143). The IMCs encoding for HIV-1 reference
415 strains AD8, JR-FL, JR-CSF, NL4-3, YU-2 were described elsewhere (144-149). HIV-1 group O
416 (RBF206), SIVcpz (TAN2) and chimeric SIVmac/HIV-1 IMC constructs ($SHIV_{AD8\text{-}EO}$ and
417 SHIV.AE.40100) were generated as previously published (150-153). CH058 IMCs defective for
418 Vpu and/or Nef expression were previously described (58). To generate a *nef*-defective JR-FL
419 IMC, a frameshift mutation was introduced at the unique XhoI restriction site within the *nef*
420 gene, resulting in a premature stop codon at position 47. To generate *vpu*-defective JR-FL IMCs,
421 two stop-codons were introduced directly after the start-codon of *vpu* using the QuikChange II
422 XL site-directed mutagenesis protocol (Agilent Technologies, Santa Clara, CA). The presence of
423 the desired mutations was determined by automated DNA sequencing. Proviral constructs,
424 collectively referred as Env-IMCs, comprising an HIV-1 NL4.3-based isogenic backbone

bioRxiv preprint doi: https://doi.org/10.1101/2021.11.03.467116; this version posted November 8, 2021. The copyright holder for this preprint (which was not certified by peer review) is the author/funder. All rights reserved. No reuse allowed without permission.

425 engineered for the insertion of heterologous *env* strain sequences and expression in *cis* of full-
426 length Env (pNL.CH058.ecto and pNL.YU-2.ecto), were previously described (47). In the same
427 study, isogenic proviral constructs encoding *Renilla* luciferase (LucR) followed in frame by a
428 ribosome-skipping T2A peptide intended to drive Nef expression were also reported (collectively
429 referred to as Env-IMC-LucR.T2A) (47). Construction of plasmids encoding for CH058 Vpu and
430 CH058 Nef in the pCGCG-IRES-eGFP expression vector was previously described (58, 59).
431
432 **Viral production and infections**
433 To achieve a similar level of infection in primary $CD4^+$ T cells among the different IMCs tested,
434 VSV-G-pseudotyped HIV-1 viruses were produced and titrated as previously described (120).
435 Viruses were then used to infect activated primary CD4+ T cells from healthy HIV-1 negative
436 donors by spin infection at 800 × *g* for 1 h in 96-well plates at 25 °C.
437
438 **Antibodies and plasma**
439 The following Abs were used to assess cell-surface Env staining: A32, 2G12 (NIH AIDS
440 Reagent Program) and PGT135 (IAVI). Mouse anti-human CD4 (clone OKT4; Thermo Fisher
441 Scientific, Waltham, MA, USA) and mouse anti-human BST-2 (clone RS38E, PE-Cy7-
442 conjugated; Biolegend, San Diego, CA, USA) were also used as primary antibodies for cell-
443 surface staining. Goat anti-mouse and anti-human antibodies pre-coupled to Alexa Fluor 647
444 (Invitrogen, Rockford, IL, USA) were used as secondary antibodies in flow cytometry
445 experiments. Plasma from HIV-infected individuals were collected, heat-inactivated and
446 conserved at −80 °C until use. Rabbit antisera raised against a Nef consensus protein (NIH AIDS
447 Reagent Program) or against a Vpu C-terminal peptide (69) were used as primary antibodies in

bioRxiv preprint doi: https://doi.org/10.1101/2021.11.03.467116; this version posted November 8, 2021. The copyright holder for this preprint (which was not certified by peer review) is the author/funder. All rights reserved. No reuse allowed without permission.

intracellular staining. BrillantViolet 421 (BV421)-conjugated donkey anti-rabbit antibodies (Biolegend) were used as secondary antibodies to detect Nef and Vpu antisera binding by flow cytometry. To avoid any potential cross-reactivity with the anti-rabbit secondary antibodies used for intracellular staining, mouse monoclonal antibodies were used to detect CD4 and BST-2 proteins.

Flow cytometry analysis of cell-surface and intracellular staining

Cell-surface staining of infected cells was performed as previously described (41). Binding of cell-surface HIV-1 Env by anti-Env mAbs (5 µg/mL) or HIV+ plasma (1:1000 dilution) was performed at 48h post-infection. Infected cells were then permeabilized using the Cytofix/Cytoperm Fixation/ Permeabilization Kit (BD Biosciences, Mississauga, ON, Canada) and stained intracellularly using PE-conjugated mouse anti-p24 mAb (clone KC57; Beckman Coulter, Brea, CA, USA; 1:100 dilution) in combination with Nef or Vpu rabbit antisera (1:1000 dilution). The percentage of infected cells ($p24^+$) was determined by gating on the living cell population according to a viability dye staining (Aqua Vivid; Thermo Fisher Scientific). Alternatively, intracellular staining was assessed on 293T expressing Nef or Vpu proteins. Briefly, $2x10^6$ 293T cells were transfected with 7ug of Nef or Vpu expressor with the calcium-phosphate method. At 48 h post transfection, 293T cells were stained intracellularly with rabbit antisera raised against Nef or Vpu (1:1000). Samples were acquired on an LSRII cytometer (BD Biosciences), and data analysis was performed using FlowJo v10.5.3 (Tree Star, Ashland, OR, USA).

FACS-based ADCC assay

bioRxiv preprint doi: https://doi.org/10.1101/2021.11.03.467116; this version posted November 8, 2021. The copyright holder for this preprint (which was not certified by peer review) is the author/funder. All rights reserved. No reuse allowed without permission.

Measurement of ADCC using the FACS-based assay was performed at 48h post-infection as previously described (43, 119). Briefly, HIV-1-infected primary CD4+ T cells were stained with AquaVivid viability dye and cell proliferation dye eFluor670 (Thermo Fisher Scientific) and used as target cells. Autologous PBMC effectors cells, stained with cell proliferation dye eFluor450 (Thermo Fisher Scientific), were added at an effector: target ratio of 10:1 in 96-well V-bottom plates (Corning, Corning, NY). A 1:1000 final dilution of plasma or 5µg/mL of A32 mAb was added to appropriate wells and cells were incubated for 5 min at room temperature. The plates were subsequently centrifuged for 1 min at 300 *x* g, and incubated at 37°C, 5% CO_2 for 5h before being fixed in a 2% PBS-formaldehyde solution. Samples were acquired on an LSRII cytometer (BD Biosciences) and data analysis was performed using FlowJo v10.5.3 (Tree Star). The percentage of ADCC was calculated with the following formula: (% of p24+ cells in Targets plus Effectors) − (% of p24+ cells in Targets plus Effectors plus plasma) / (% of p24+ cells in Targets) by gating on infected lived target cells.

Software Scripts and Visualization

Correlograms were generated using the corrplot package in program R v.4.1.012 and RStudio v.1.4.1106 (154, 155) . Correlation networks were created using the ggraph and igraph packages in R in undirected mode, clustered based on the igraph layout “star”. Edges are weighted according to P-values (inversely). Edges are only shown if $P < 0.05$, and nodes without edges were removed. Nodes are sized according to the r-values of connecting edges. Multiple linear regression analyses were performed using the GraphPad Prism software (version 9.1.0). The coefficient of determination (R^2) was used as a metric to measure the proportion of the variation observed with the dependant variable that can be explained by the variation in the independent

bioRxiv preprint doi: https://doi.org/10.1101/2021.11.03.467116; this version posted November 8, 2021. The copyright holder for this preprint (which was not certified by peer review) is the author/funder. All rights reserved. No reuse allowed without permission.

494 variables. Since R^2 values usually increases when more predictive variables are added to the
495 model, we also measured the adjusted R^2 (adj. R^2) to account for this caveat.
496
497 **Statistical analysis**
498 Statistics were analyzed using GraphPad Prism version 9.1.0 (GraphPad, San Diego, CA, USA).
499 Every data set was tested for statistical normality and this information was used to apply the
500 appropriate (parametric or nonparametric) statistical test. P values <0.05 were considered
501 significant; significance values are indicated as * $P<0.05$, ** $P<0.01$, *** $P<0.001$, ****
502 $P<0.0001$.
503

bioRxiv preprint doi: https://doi.org/10.1101/2021.11.03.467116; this version posted November 8, 2021. The copyright holder for this preprint (which was not certified by peer review) is the author/funder. All rights reserved. No reuse allowed without permission.

FIGURE LEGENDS

Figure 1. Intracellular detection of Nef and Vpu in infected primary CD4+ T cells.

(**A-C**) 293T cells transfected with an empty vector or a plasmid expressing either CH058 Nef or CH058 Vpu. 48 hours post-transfection, cells were permeabilized and stained with rabbit polyclonal antisera raised against Nef and Vpu to detect their respective intracellular expression. Antiserum binding was detected using donkey anti-rabbit BV421 secondary Abs. (**A**) Histograms depicting representative staining and (**B-C**) Median fluorescence intensities (MFI) obtained for multiple independent stainings using (**B**) anti-Nef or (**C**) anti-Vpu. (**D-G**) Primary CD4+T cells mock-infected or infected with CH058 T/F WT, Nef- or Vpu-, were stained to detect the intracellular expression of Nef or Vpu. (**D,F**) Dot plots (left) and histograms (right) depicting representative (**D**) Nef and (**F**) Vpu staining. (**E,G**) The graphs show the MFI obtained from different cell populations using cells from five different donors using (**E**) anti-Nef or (**G**) anti-Vpu. Error bars indicate means ± standard errors of the means (SEM). Statistical significance was tested using an unpaired t test or a Mann-Whitney U test based on statistical normality (*, $P < 0.05$; **, $P < 0.01$; ***, $P < 0.001$; ns, nonsignificant). (**H-I**) Primary CD4+ T cells were infected with a panel of viruses from different clades (A1, B, C, CRF01_AE), group (M, O) and host (HIV-1, SIVcpz, SHIV). The radar plots indicate the level of specific recognition of infected cells (MFI normalized to uninfected cells) using the (**H**) anti-Nef or (**I**) anti-Vpu antisera. The limit of detection was determined using (**H**) cells infected with CH058 Nef- for Nef staining and using (**I**) cells infected with CH058 Vpu- for Vpu staining.

bioRxiv preprint doi: https://doi.org/10.1101/2021.11.03.467116; this version posted November 8, 2021. The copyright holder for this preprint (which was not certified by peer review) is the author/funder. All rights reserved. No reuse allowed without permission.

Figure 2. Concomitant detection of intracellular Nef and Vpu and cell-surface CD4 and BST-2.

Primary CD4+T cells infected with CH058 T/F WT, Nef-, Vpu-, Vpu A14L/A18L or Vpu S52A/S56A viruses were stained for cell-surface CD4 and BST-2 prior to detection of intracellular Nef or Vpu expression. (**A,C,E**) Contour plots depicting representative cell-surface CD4 or BST-2 detection in combination with Nef or Vpu intracellular detection. Mock-infected cells were used as a control and are shown in grey. (**B,D,F**) The graphs show MFIs obtained from five independent experiments. Error bars indicate means ± standard errors of the means (SEM). Statistical significance was tested using an unpaired t test or a Mann-Whitney U test based on statistical normality (*, $P < 0.05$; **, $P < 0.01$; ***, $P < 0.001$; ns, nonsignificant).

Figure 3. Nef and Vpu intracellular detection inversely correlates with the recognition of infected cells and their susceptibility to ADCC responses mediated by HIV+ plasma.

Primary CD4+T cells were mock-infected (grey), infected with CH058 T/F (red) or JR-FL (Blue) viruses (WT, Nef-, Vpu-, Nef- Vpu-) and stained for (**A**) intracellular Nef or Vpu expression in combination with (**B**) cell-surface staining of Env (using the anti-Env 2G12 mAb), CD4 and BST-2. The ability of the anti-Env A32 mAb and 25 different HIV+ plasma to (**C**) recognize infected cells and (**D**) eliminate infected cells by ADCC was also measured. (**A-D**) The graphs show the MFI obtained on the infected (p24+) cell population using cells from five different donors. Error bars indicate means ± standard errors of the means (SEM). Statistical significance was tested using an unpaired t test or a Mann-Whitney U test based on statistical normality (*, $P < 0.05$; **, $P < 0.01$; ***, $P < 0.001$; ns, nonsignificant). (**E**) Correlograms summarize pairwise correlations among all immunological, virological and cellular variables obtained from infected

bioRxiv preprint doi: https://doi.org/10.1101/2021.11.03.467116; this version posted November 8, 2021. The copyright holder for this preprint (which was not certified by peer review) is the author/funder. All rights reserved. No reuse allowed without permission.

549 primary CD4+ T cells (shown in A-D). Squares are color-coded according to the magnitude of
550 the correlation coefficient (r) and the square dimensions are inversely proportional with the P-
551 values. Red squares represent a positive correlation between two variables and blue squares
552 represent negative correlations. Asterisks indicate all statistically significant correlations (*P <
553 0.05, **P < 0.01, ***P < 0.005). Correlation analysis was done using nonparametric Spearman
554 rank tests. (**F**) Correlation networks were generated using data shown in (**E**). Each node (circle)
555 represents a cellular (red), an immunological (green) or a virological (blue) feature measured on
556 infected cells. Nodes are connected with edges (lines) if they are significantly correlated (P <
557 0.05); nodes without edges were removed. Edges are weighted according to P-values (inversely).
558 Red edges represent a positive correlation between two variables and blue edges represent
559 negative correlations. Nodes are sized according to the r-values of connecting edges.
560
561 **Figure 4. Lack of Nef expression in primary CD4+ T cells infected with LucR.T2A IMCs**
562 **results in enhanced ADCC.**
563 Primary CD4+T cells mock-infected (grey) or infected with chimeric IMCs expressing CH058
564 Env (red) or YU-2 Env (green) and expressing or not the LucR reporter gene. (**A**) Dot plots
565 depicting representative stainings of intracellular Nef or Vpu expression. (**B-C**) Detection by
566 flow cytometry of (**B**) intracellular Nef or Vpu expression in combination with (**C**) cell-surface
567 staining of Env (using anti-Env mAbs 2G12 (CH058) or PGT135 (YU-2)), CD4 and BST-2. The
568 ability of the A32 mAb and 25 HIV+ plasma to (**D**) recognize infected cells and (**E**) eliminate
569 infected cells by ADCC was also measured. (**B-E**) The graphs show the MFI obtained on the
570 infected (p24+) cell population using cells from five different donors. Error bars indicate means
571 ± standard errors of the means (SEM). Statistical significance was tested using an unpaired t test

bioRxiv preprint doi: https://doi.org/10.1101/2021.11.03.467116; this version posted November 8, 2021. The copyright holder for this preprint (which was not certified by peer review) is the author/funder. All rights reserved. No reuse allowed without permission.

572 or a Mann-Whitney U test based on statistical normality (*, $P < 0.05$; **, $P < 0.01$; ***,
573 $P < 0.001$; ns, nonsignificant). (**F**) Correlograms summarize pairwise correlations among all
574 immunological, virological and cellular variables obtained from infected primary CD4+ T cells
575 (shown in **B-E**). Squares are color-coded according to the magnitude of the correlation
576 coefficient (r) and the square dimensions are inversely proportional with the P-values. Red
577 squares represent a positive correlation between two variables and blue squares represent
578 negative correlations. Asterisks indicate all statistically significant correlations (*$P < 0.05$, **$P <$
579 0.01, ***$P < 0.005$). Correlation analysis was done using nonparametric Spearman rank tests.
580 (**G**) Correlation networks were generated using data shown in (**F**). Each node (circle) represents
581 a cellular (red), an immunological (green) or a virological (blue) feature measured on infected
582 cells. Nodes are connected with edges (lines) if they are significantly correlated ($P < 0.05$); nodes
583 without edges were removed. Edges are weighted according to P-values (inversely). Red edges
584 represent a positive correlation between two variables and blue edges represent negative
585 correlations. Nodes are sized according to the r-values of connecting edges.
586
587 **Figure 5. Prediction of ADCC responses mediated by HIV+ plasma using multiple linear**
588 **regression models.**
589 (**A-C**) Multiple linear regression analysis to identify variables that can predict the ADCC
590 responses mediated by HIV+ plasma against primary CD4+ T cells infected by different viral
591 constructs (WT, Nef-, Vpu-, Nef-Vpu-, Env-IMC, Env-IMC-LucR.T2A) from different HIV-1
592 strains (CH058, JR-FL, YU-2). Each dot represents a single virus where the average of ADCC
593 obtained with 25 different HIV+ plasma (dependent variable) is plotted on the X axis and the
594 predicted ADCC value based on one or more independent parameters is plotted on the Y axis.

bioRxiv preprint doi: https://doi.org/10.1101/2021.11.03.467116; this version posted November 8, 2021. The copyright holder for this preprint (which was not certified by peer review) is the author/funder. All rights reserved. No reuse allowed without permission.

595 Predictors include (**A**) cellular variables, (**B**) virological variables and (**C**) immunological
596 variables. Multiple linear regression analyses were performed using the GraphPad Prism
597 software (version 9.1.0). P values below 0.05 are considered significant and are highlighted in
598 bold. The coefficient of multiple correlation (R^2) indicates the goodness of fit of the multiple
599 regression linear model. The adjusted R^2 (Adj. R^2) is used to compare the fits of models across
600 experiments with different numbers of data points and independent variables.
601
602

bioRxiv preprint doi: https://doi.org/10.1101/2021.11.03.467116; this version posted November 8, 2021. The copyright holder for this preprint (which was not certified by peer review) is the author/funder. All rights reserved. No reuse allowed without permission.

REFERENCES

1. Desrosiers RC, Lifson JD, Gibbs JS, Czajak SC, Howe AY, Arthur LO, Johnson RP. 1998. Identification of highly attenuated mutants of simian immunodeficiency virus. J Virol 72:1431-7.
2. Dave VP, Hajjar F, Dieng MM, Haddad E, Cohen EA. 2013. Efficient BST2 antagonism by Vpu is critical for early HIV-1 dissemination in humanized mice. Retrovirology 10:128.
3. Sato K, Misawa N, Fukuhara M, Iwami S, An DS, Ito M, Koyanagi Y. 2012. Vpu augments the initial burst phase of HIV-1 propagation and downregulates BST2 and CD4 in humanized mice. J Virol 86:5000-13.
4. Sato K, Misawa N, Iwami S, Satou Y, Matsuoka M, Ishizaka Y, Ito M, Aihara K, An DS, Koyanagi Y. 2013. HIV-1 Vpr accelerates viral replication during acute infection by exploitation of proliferating CD4+ T cells in vivo. PLoS Pathog 9:e1003812.
5. Crotti A, Neri F, Corti D, Ghezzi S, Heltai S, Baur A, Poli G, Santagostino E, Vicenzi E. 2006. Nef alleles from human immunodeficiency virus type 1-infected long-term-nonprogressor hemophiliacs with or without late disease progression are defective in enhancing virus replication and CD4 down-regulation. J Virol 80:10663-74.
6. Rucker E, Grivel JC, Munch J, Kirchhoff F, Margolis L. 2004. Vpr and Vpu are important for efficient human immunodeficiency virus type 1 replication and CD4+ T-cell depletion in human lymphoid tissue ex vivo. J Virol 78:12689-93.
7. Kirchhoff F, Greenough TC, Brettler DB, Sullivan JL, Desrosiers RC. 1995. Brief report: absence of intact nef sequences in a long-term survivor with nonprogressive HIV-1 infection. N Engl J Med 332:228-32.
8. Haller C, Muller B, Fritz JV, Lamas-Murua M, Stolp B, Pujol FM, Keppler OT, Fackler OT. 2014. HIV-1 Nef and Vpu are functionally redundant broad-spectrum modulators of cell surface receptors, including tetraspanins. J Virol 88:14241-57.
9. Tokarev A, Guatelli J. 2011. Misdirection of membrane trafficking by HIV-1 Vpu and Nef: Keys to viral virulence and persistence. Cell Logist 1:90-102.
10. Purcell DF, Martin MA. 1993. Alternative splicing of human immunodeficiency virus type 1 mRNA modulates viral protein expression, replication, and infectivity. J Virol 67:6365-78.
11. Bentham M, Mazaleyrat S, Harris M. 2006. Role of myristoylation and N-terminal basic residues in membrane association of the human immunodeficiency virus type 1 Nef protein. J Gen Virol 87:563-571.
12. Craig HM, Reddy TR, Riggs NL, Dao PP, Guatelli JC. 2000. Interactions of HIV-1 nef with the mu subunits of adaptor protein complexes 1, 2, and 3: role of the dileucine-based sorting motif. Virology 271:9-17.
13. Chaudhuri R, Lindwasser OW, Smith WJ, Hurley JH, Bonifacino JS. 2007. Downregulation of CD4 by human immunodeficiency virus type 1 Nef is dependent on clathrin and involves direct interaction of Nef with the AP2 clathrin adaptor. J Virol 81:3877-90.
14. Ren X, Park SY, Bonifacino JS, Hurley JH. 2014. How HIV-1 Nef hijacks the AP-2 clathrin adaptor to downregulate CD4. Elife 3:e01754.
15. Aiken C, Konner J, Landau NR, Lenburg ME, Trono D. 1994. Nef induces CD4 endocytosis: requirement for a critical dileucine motif in the membrane-proximal CD4 cytoplasmic domain. Cell 76:853-64.
16. Rhee SS, Marsh JW. 1994. Human immunodeficiency virus type 1 Nef-induced down-modulation of CD4 is due to rapid internalization and degradation of surface CD4. J Virol 68:5156-63.

bioRxiv preprint doi: https://doi.org/10.1101/2021.11.03.467116; this version posted November 8, 2021. The copyright holder for this preprint (which was not certified by peer review) is the author/funder. All rights reserved. No reuse allowed without permission.

17. Schwartz S, Felber BK, Pavlakis GN. 1992. Mechanism of translation of monocistronic and multicistronic human immunodeficiency virus type 1 mRNAs. Mol Cell Biol 12:207-19.
18. Krummheuer J, Johnson AT, Hauber I, Kammler S, Anderson JL, Hauber J, Purcell DF, Schaal H. 2007. A minimal uORF within the HIV-1 vpu leader allows efficient translation initiation at the downstream env AUG. Virology 363:261-71.
19. Wray V, Federau T, Henklein P, Klabunde S, Kunert O, Schomburg D, Schubert U. 1995. Solution structure of the hydrophilic region of HIV-1 encoded virus protein U (Vpu) by CD and 1H NMR spectroscopy. Int J Pept Protein Res 45:35-43.
20. Maldarelli F, Chen MY, Willey RL, Strebel K. 1993. Human immunodeficiency virus type 1 Vpu protein is an oligomeric type I integral membrane protein. J Virol 67:5056-61.
21. Marassi FM, Ma C, Gratkowski H, Straus SK, Strebel K, Oblatt-Montal M, Montal M, Opella SJ. 1999. Correlation of the structural and functional domains in the membrane protein Vpu from HIV-1. Proc Natl Acad Sci U S A 96:14336-41.
22. Margottin F, Bour SP, Durand H, Selig L, Benichou S, Richard V, Thomas D, Strebel K, Benarous R. 1998. A novel human WD protein, h-beta TrCp, that interacts with HIV-1 Vpu connects CD4 to the ER degradation pathway through an F-box motif. Mol Cell 1:565-74.
23. Coadou G, Evrard-Todeschi N, Gharbi-Benarous J, Benarous R, Girault JP. 2002. HIV-1 encoded virus protein U (Vpu) solution structure of the 41-62 hydrophilic region containing the phosphorylated sites Ser52 and Ser56. Int J Biol Macromol 30:23-40.
24. Dube M, Roy BB, Guiot-Guillain P, Mercier J, Binette J, Leung G, Cohen EA. 2009. Suppression of Tetherin-restricting activity upon human immunodeficiency virus type 1 particle release correlates with localization of Vpu in the trans-Golgi network. J Virol 83:4574-90.
25. Klimkait T, Strebel K, Hoggan MD, Martin MA, Orenstein JM. 1990. The human immunodeficiency virus type 1-specific protein vpu is required for efficient virus maturation and release. J Virol 64:621-9.
26. Schubert U, Strebel K. 1994. Differential activities of the human immunodeficiency virus type 1-encoded Vpu protein are regulated by phosphorylation and occur in different cellular compartments. J Virol 68:2260-71.
27. Schubert U, Anton LC, Bacik I, Cox JH, Bour S, Bennink JR, Orlowski M, Strebel K, Yewdell JW. 1998. CD4 glycoprotein degradation induced by human immunodeficiency virus type 1 Vpu protein requires the function of proteasomes and the ubiquitin-conjugating pathway. J Virol 72:2280-8.
28. Willey RL, Maldarelli F, Martin MA, Strebel K. 1992. Human immunodeficiency virus type 1 Vpu protein induces rapid degradation of CD4. J Virol 66:7193-200.
29. Magadan JG, Perez-Victoria FJ, Sougrat R, Ye Y, Strebel K, Bonifacino JS. 2010. Multilayered mechanism of CD4 downregulation by HIV-1 Vpu involving distinct ER retention and ERAD targeting steps. PLoS Pathog 6:e1000869.
30. Neil SJ, Zang T, Bieniasz PD. 2008. Tetherin inhibits retrovirus release and is antagonized by HIV-1 Vpu. Nature 451:425-30.
31. Van Damme N, Goff D, Katsura C, Jorgenson RL, Mitchell R, Johnson MC, Stephens EB, Guatelli J. 2008. The interferon-induced protein BST-2 restricts HIV-1 release and is downregulated from the cell surface by the viral Vpu protein. Cell Host Microbe 3:245-52.
32. Dube M, Roy BB, Guiot-Guillain P, Binette J, Mercier J, Chiasson A, Cohen EA. 2010. Antagonism of tetherin restriction of HIV-1 release by Vpu involves binding and sequestration of the restriction factor in a perinuclear compartment. PLoS Pathog 6:e1000856.

bioRxiv preprint doi: https://doi.org/10.1101/2021.11.03.467116; this version posted November 8, 2021. The copyright holder for this preprint (which was not certified by peer review) is the author/funder. All rights reserved. No reuse allowed without permission.

33. Hauser H, Lopez LA, Yang SJ, Oldenburg JE, Exline CM, Guatelli JC, Cannon PM. 2010. HIV-1 Vpu and HIV-2 Env counteract BST-2/tetherin by sequestration in a perinuclear compartment. Retrovirology 7:51.
34. Wildum S, Schindler M, Munch J, Kirchhoff F. 2006. Contribution of Vpu, Env, and Nef to CD4 down-modulation and resistance of human immunodeficiency virus type 1-infected T cells to superinfection. J Virol 80:8047-59.
35. Ding S, Gasser R, Gendron-Lepage G, Medjahed H, Tolbert WD, Sodroski J, Pazgier M, Finzi A. 2019. CD4 Incorporation into HIV-1 Viral Particles Exposes Envelope Epitopes Recognized by CD4-Induced Antibodies. J Virol 93.
36. Bour S, Perrin C, Strebel K. 1999. Cell surface CD4 inhibits HIV-1 particle release by interfering with Vpu activity. J Biol Chem 274:33800-6.
37. Cortes MJ, Wong-Staal F, Lama J. 2002. Cell surface CD4 interferes with the infectivity of HIV-1 particles released from T cells. J Biol Chem 277:1770-9.
38. Lama J, Mangasarian A, Trono D. 1999. Cell-surface expression of CD4 reduces HIV-1 infectivity by blocking Env incorporation in a Nef- and Vpu-inhibitable manner. Curr Biol 9:622-31.
39. Levesque K, Zhao YS, Cohen EA. 2003. Vpu exerts a positive effect on HIV-1 infectivity by down-modulating CD4 receptor molecules at the surface of HIV-1-producing cells. J Biol Chem 278:28346-53.
40. Decker JM, Bibollet-Ruche F, Wei X, Wang S, Levy DN, Wang W, Delaporte E, Peeters M, Derdeyn CA, Allen S, Hunter E, Saag MS, Hoxie JA, Hahn BH, Kwong PD, Robinson JE, Shaw GM. 2005. Antigenic conservation and immunogenicity of the HIV coreceptor binding site. J Exp Med 201:1407-19.
41. Veillette M, Coutu M, Richard J, Batraville LA, Dagher O, Bernard N, Tremblay C, Kaufmann DE, Roger M, Finzi A. 2015. The HIV-1 gp120 CD4-Bound Conformation Is Preferentially Targeted by Antibody-Dependent Cellular Cytotoxicity-Mediating Antibodies in Sera from HIV-1-Infected Individuals. J Virol 89:545-51.
42. Guan Y, Pazgier M, Sajadi MM, Kamin-Lewis R, Al-Darmarki S, Flinko R, Lovo E, Wu X, Robinson JE, Seaman MS, Fouts TR, Gallo RC, DeVico AL, Lewis GK. 2013. Diverse specificity and effector function among human antibodies to HIV-1 envelope glycoprotein epitopes exposed by CD4 binding. Proc Natl Acad Sci U S A 110:E69-78.
43. Veillette M, Desormeaux A, Medjahed H, Gharsallah NE, Coutu M, Baalwa J, Guan Y, Lewis G, Ferrari G, Hahn BH, Haynes BF, Robinson JE, Kaufmann DE, Bonsignori M, Sodroski J, Finzi A. 2014. Interaction with cellular CD4 exposes HIV-1 envelope epitopes targeted by antibody-dependent cell-mediated cytotoxicity. J Virol 88:2633-44.
44. Alsahafi N, Ding S, Richard J, Markle T, Brassard N, Walker B, Lewis GK, Kaufmann DE, Brockman MA, Finzi A. 2016. Nef Proteins from HIV-1 Elite Controllers Are Inefficient at Preventing Antibody-Dependent Cellular Cytotoxicity. J Virol 90:2993-3002.
45. Schaefer MR, Wonderlich ER, Roeth JF, Leonard JA, Collins KL. 2008. HIV-1 Nef targets MHC-I and CD4 for degradation via a final common beta-COP-dependent pathway in T cells. PLoS Pathog 4:e1000131.
46. Dikeakos JD, Atkins KM, Thomas L, Emert-Sedlak L, Byeon IJ, Jung J, Ahn J, Wortman MD, Kukull B, Saito M, Koizumi H, Williamson DM, Hiyoshi M, Barklis E, Takiguchi M, Suzu S, Gronenborn AM, Smithgall TE, Thomas G. 2010. Small molecule inhibition of HIV-1-induced MHC-I down-regulation identifies a temporally regulated switch in Nef action. Mol Biol Cell 21:3279-92.
47. Edmonds TG, Ding H, Yuan X, Wei Q, Smith KS, Conway JA, Wieczorek L, Brown B, Polonis V, West JT, Montefiori DC, Kappes JC, Ochsenbauer C. 2010. Replication competent molecular clones of HIV-1 expressing Renilla luciferase facilitate the analysis of antibody inhibition in PBMC. Virology 408:1-13.

bioRxiv preprint doi: https://doi.org/10.1101/2021.11.03.467116; this version posted November 8, 2021. The copyright holder for this preprint (which was not certified by peer review) is the author/funder. All rights reserved. No reuse allowed without permission.

48. Atkins KM, Thomas L, Youker RT, Harriff MJ, Pissani F, You H, Thomas G. 2008. HIV-1 Nef binds PACS-2 to assemble a multikinase cascade that triggers major histocompatibility complex class I (MHC-I) down-regulation: analysis using short interfering RNA and knock-out mice. J Biol Chem 283:11772-84.
49. Lenassi M, Cagney G, Liao M, Vaupotic T, Bartholomeeusen K, Cheng Y, Krogan NJ, Plemenitas A, Peterlin BM. 2010. HIV Nef is secreted in exosomes and triggers apoptosis in bystander CD4+ T cells. Traffic 11:110-22.
50. Komoto S, Tsuji S, Ibrahim MS, Li YG, Warachit J, Taniguchi K, Ikuta K. 2003. The vpu protein of human immunodeficiency virus type 1 plays a protective role against virus-induced apoptosis in primary CD4(+) T lymphocytes. J Virol 77:10304-13.
51. Miyagi E, Andrew AJ, Kao S, Strebel K. 2009. Vpu enhances HIV-1 virus release in the absence of Bst-2 cell surface down-modulation and intracellular depletion. Proc Natl Acad Sci U S A 106:2868-73.
52. Chu H, Wang JJ, Qi M, Yoon JJ, Chen X, Wen X, Hammonds J, Ding L, Spearman P. 2012. Tetherin/BST-2 is essential for the formation of the intracellular virus-containing compartment in HIV-infected macrophages. Cell Host Microbe 12:360-72.
53. Shugars DC, Smith MS, Glueck DH, Nantermet PV, Seillier-Moiseiwitsch F, Swanstrom R. 1993. Analysis of human immunodeficiency virus type 1 nef gene sequences present in vivo. J Virol 67:4639-50.
54. Alberti MO, Jones JJ, Miglietta R, Ding H, Bakshi RK, Edmonds TG, Kappes JC, Ochsenbauer C. 2015. Optimized Replicating Renilla Luciferase Reporter HIV-1 Utilizing Novel Internal Ribosome Entry Site Elements for Native Nef Expression and Function. AIDS Res Hum Retroviruses 31:1278-96.
55. Jacob RA, Edgar CR, Prevost J, Trothen SM, Lurie A, Mumby MJ, Galbraith A, Kirchhoff F, Haeryfar SMM, Finzi A, Dikeakos JD. 2021. The HIV-1 accessory protein Nef increases surface expression of the checkpoint receptor Tim-3 in infected CD4(+) T cells. J Biol Chem 297:101042.
56. Pawlak EN, Dirk BS, Jacob RA, Johnson AL, Dikeakos JD. 2018. The HIV-1 accessory proteins Nef and Vpu downregulate total and cell surface CD28 in CD4(+) T cells. Retrovirology 15:6.
57. Cohen EA, Terwilliger EF, Sodroski JG, Haseltine WA. 1988. Identification of a protein encoded by the vpu gene of HIV-1. Nature 334:532-4.
58. Heigele A, Kmiec D, Regensburger K, Langer S, Peiffer L, Sturzel CM, Sauter D, Peeters M, Pizzato M, Learn GH, Hahn BH, Kirchhoff F. 2016. The Potency of Nef-Mediated SERINC5 Antagonism Correlates with the Prevalence of Primate Lentiviruses in the Wild. Cell Host Microbe 20:381-91.
59. Kmiec D, Iyer SS, Sturzel CM, Sauter D, Hahn BH, Kirchhoff F. 2016. Vpu-Mediated Counteraction of Tetherin Is a Major Determinant of HIV-1 Interferon Resistance. MBio 7.
60. Bolduan S, Hubel P, Reif T, Lodermeyer V, Hohne K, Fritz JV, Sauter D, Kirchhoff F, Fackler OT, Schindler M, Schubert U. 2013. HIV-1 Vpu affects the anterograde transport and the glycosylation pattern of NTB-A. Virology 440:190-203.
61. Bolduan S, Reif T, Schindler M, Schubert U. 2014. HIV-1 Vpu mediated downregulation of CD155 requires alanine residues 10, 14 and 18 of the transmembrane domain. Virology 464-465:375-384.
62. Vassena L, Giuliani E, Koppensteiner H, Bolduan S, Schindler M, Doria M. 2015. HIV-1 Nef and Vpu Interfere with L-Selectin (CD62L) Cell Surface Expression To Inhibit Adhesion and Signaling in Infected CD4+ T Lymphocytes. J Virol 89:5687-700.
63. Prevost J, Pickering S, Mumby MJ, Medjahed H, Gendron-Lepage G, Delgado GG, Dirk BS, Dikeakos JD, Sturzel CM, Sauter D, Kirchhoff F, Bibollet-Ruche F, Hahn BH, Dube M, Kaufmann DE, Neil SJD, Finzi A, Richard J. 2019. Upregulation of BST-2 by Type I

bioRxiv preprint doi: https://doi.org/10.1101/2021.11.03.467116; this version posted November 8, 2021. The copyright holder for this preprint (which was not certified by peer review) is the author/funder. All rights reserved. No reuse allowed without permission.

Interferons Reduces the Capacity of Vpu To Protect HIV-1-Infected Cells from NK Cell Responses. mBio 10.

64. Bour S, Schubert U, Strebel K. 1995. The human immunodeficiency virus type 1 Vpu protein specifically binds to the cytoplasmic domain of CD4: implications for the mechanism of degradation. J Virol 69:1510-20.
65. Chen MY, Maldarelli F, Karczewski MK, Willey RL, Strebel K. 1993. Human immunodeficiency virus type 1 Vpu protein induces degradation of CD4 in vitro: the cytoplasmic domain of CD4 contributes to Vpu sensitivity. J Virol 67:3877-84.
66. Lenburg ME, Landau NR. 1993. Vpu-induced degradation of CD4: requirement for specific amino acid residues in the cytoplasmic domain of CD4. J Virol 67:7238-45.
67. Vincent MJ, Raja NU, Jabbar MA. 1993. Human immunodeficiency virus type 1 Vpu protein induces degradation of chimeric envelope glycoproteins bearing the cytoplasmic and anchor domains of CD4: role of the cytoplasmic domain in Vpu-induced degradation in the endoplasmic reticulum. J Virol 67:5538-49.
68. Margottin F, Benichou S, Durand H, Richard V, Liu LX, Gomas E, Benarous R. 1996. Interaction between the cytoplasmic domains of HIV-1 Vpu and CD4: role of Vpu residues involved in CD4 interaction and in vitro CD4 degradation. Virology 223:381-6.
69. Prevost J, Edgar CR, Richard J, Trothen SM, Jacob RA, Mumby MJ, Pickering S, Dube M, Kaufmann DE, Kirchhoff F, Neil SJD, Finzi A, Dikeakos JD. 2020. HIV-1 Vpu Downregulates Tim-3 from the Surface of Infected CD4(+) T Cells. J Virol 94.
70. Binette J, Dube M, Mercier J, Halawani D, Latterich M, Cohen EA. 2007. Requirements for the selective degradation of CD4 receptor molecules by the human immunodeficiency virus type 1 Vpu protein in the endoplasmic reticulum. Retrovirology 4:75.
71. Mitchell RS, Katsura C, Skasko MA, Fitzpatrick K, Lau D, Ruiz A, Stephens EB, Margottin-Goguet F, Benarous R, Guatelli JC. 2009. Vpu antagonizes BST-2-mediated restriction of HIV-1 release via beta-TrCP and endo-lysosomal trafficking. PLoS Pathog 5:e1000450.
72. Gustin JK, Douglas JL, Bai Y, Moses AV. 2012. Ubiquitination of BST-2 protein by HIV-1 Vpu protein does not require lysine, serine, or threonine residues within the BST-2 cytoplasmic domain. J Biol Chem 287:14837-50.
73. Belaidouni N, Marchal C, Benarous R, Besnard-Guerin C. 2007. Involvement of the betaTrCP in the ubiquitination and stability of the HIV-1 Vpu protein. Biochem Biophys Res Commun 357:688-93.
74. Kueck T, Neil SJ. 2012. A cytoplasmic tail determinant in HIV-1 Vpu mediates targeting of tetherin for endosomal degradation and counteracts interferon-induced restriction. PLoS Pathog 8:e1002609.
75. Kueck T, Foster TL, Weinelt J, Sumner JC, Pickering S, Neil SJ. 2015. Serine Phosphorylation of HIV-1 Vpu and Its Binding to Tetherin Regulates Interaction with Clathrin Adaptors. PLoS Pathog 11:e1005141.
76. Mangeat B, Gers-Huber G, Lehmann M, Zufferey M, Luban J, Piguet V. 2009. HIV-1 Vpu neutralizes the antiviral factor Tetherin/BST-2 by binding it and directing its beta-TrCP2-dependent degradation. PLoS Pathog 5:e1000574.
77. Arias JF, Heyer LN, von Bredow B, Weisgrau KL, Moldt B, Burton DR, Rakasz EG, Evans DT. 2014. Tetherin antagonism by Vpu protects HIV-infected cells from antibody-dependent cell-mediated cytotoxicity. Proc Natl Acad Sci U S A 111:6425-30.
78. Alvarez RA, Hamlin RE, Monroe A, Moldt B, Hotta MT, Rodriguez Caprio G, Fierer DS, Simon V, Chen BK. 2014. HIV-1 Vpu antagonism of tetherin inhibits antibody-dependent cellular cytotoxic responses by natural killer cells. J Virol 88:6031-46.

bioRxiv preprint doi: https://doi.org/10.1101/2021.11.03.467116; this version posted November 8, 2021. The copyright holder for this preprint (which was not certified by peer review) is the author/funder. All rights reserved. No reuse allowed without permission.

79. Prevost J, Richard J, Medjahed H, Alexander A, Jones J, Kappes JC, Ochsenbauer C, Finzi A. 2018. Incomplete Downregulation of CD4 Expression Affects HIV-1 Env Conformation and Antibody-Dependent Cellular Cytotoxicity Responses. J Virol 92.
80. Ding S, Veillette M, Coutu M, Prevost J, Scharf L, Bjorkman PJ, Ferrari G, Robinson JE, Sturzel C, Hahn BH, Sauter D, Kirchhoff F, Lewis GK, Pazgier M, Finzi A. 2016. A Highly Conserved Residue of the HIV-1 gp120 Inner Domain Is Important for Antibody-Dependent Cellular Cytotoxicity Responses Mediated by Anti-cluster A Antibodies. J Virol 90:2127-34.
81. Ferrari G, Pollara J, Kozink D, Harms T, Drinker M, Freel S, Moody MA, Alam SM, Tomaras GD, Ochsenbauer C, Kappes JC, Shaw GM, Hoxie JA, Robinson JE, Haynes BF. 2011. An HIV-1 gp120 envelope human monoclonal antibody that recognizes a C1 conformational epitope mediates potent antibody-dependent cellular cytotoxicity (ADCC) activity and defines a common ADCC epitope in human HIV-1 serum. J Virol 85:7029-36.
82. Tomaras GD, Ferrari G, Shen X, Alam SM, Liao HX, Pollara J, Bonsignori M, Moody MA, Fong Y, Chen X, Poling B, Nicholson CO, Zhang R, Lu X, Parks R, Kaewkungwal J, Nitayaphan S, Pitisuttithum P, Rerks-Ngarm S, Gilbert PB, Kim JH, Michael NL, Montefiori DC, Haynes BF. 2013. Vaccine-induced plasma IgA specific for the C1 region of the HIV-1 envelope blocks binding and effector function of IgG. Proc Natl Acad Sci U S A doi:10.1073/pnas.1301456110.
83. Pollara J, Bonsignori M, Moody MA, Liu P, Alam SM, Hwang KK, Gurley TC, Kozink DM, Armand LC, Marshall DJ, Whitesides JF, Kaewkungwal J, Nitayaphan S, Pitisuttithum P, Rerks-Ngarm S, Robb ML, O'Connell RJ, Kim JH, Michael NL, Montefiori DC, Tomaras GD, Liao HX, Haynes BF, Ferrari G. 2014. HIV-1 vaccine-induced C1 and V2 Env-specific antibodies synergize for increased antiviral activities. J Virol 88:7715-26.
84. Santra S, Tomaras GD, Warrier R, Nicely NI, Liao HX, Pollara J, Liu P, Alam SM, Zhang R, Cocklin SL, Shen X, Duffy R, Xia SM, Schutte RJ, Pemble Iv CW, Dennison SM, Li H, Chao A, Vidnovic K, Evans A, Klein K, Kumar A, Robinson J, Landucci G, Forthal DN, Montefiori DC, Kaewkungwal J, Nitayaphan S, Pitisuttithum P, Rerks-Ngarm S, Robb ML, Michael NL, Kim JH, Soderberg KA, Giorgi EE, Blair L, Korber BT, Moog C, Shattock RJ, Letvin NL, Schmitz JE, Moody MA, Gao F, Ferrari G, Shaw GM, Haynes BF. 2015. Human Non-neutralizing HIV-1 Envelope Monoclonal Antibodies Limit the Number of Founder Viruses during SHIV Mucosal Infection in Rhesus Macaques. PLoS Pathog 11:e1005042.
85. Huang Y, Ferrari G, Alter G, Forthal DN, Kappes JC, Lewis GK, Love JC, Borate B, Harris L, Greene K, Gao H, Phan TB, Landucci G, Goods BA, Dowell KG, Cheng HD, Bailey-Kellogg C, Montefiori DC, Ackerman ME. 2016. Diversity of Antiviral IgG Effector Activities Observed in HIV-Infected and Vaccinated Subjects. J Immunol 197:4603-4612.
86. Costa MR, Pollara J, Edwards RW, Seaman MS, Gorny MK, Montefiori DC, Liao HX, Ferrari G, Lu S, Wang S. 2016. Fc Receptor-Mediated Activities of Env-Specific Human Monoclonal Antibodies Generated from Volunteers Receiving the DNA Prime-Protein Boost HIV Vaccine DP6-001. J Virol 90:10362-10378.
87. Bradley T, Pollara J, Santra S, Vandergrift N, Pittala S, Bailey-Kellogg C, Shen X, Parks R, Goodman D, Eaton A, Balachandran H, Mach LV, Saunders KO, Weiner JA, Scearce R, Sutherland LL, Phogat S, Tartaglia J, Reed SG, Hu SL, Theis JF, Pinter A, Montefiori DC, Kepler TB, Peachman KK, Rao M, Michael NL, Suscovich TJ, Alter G, Ackerman ME, Moody MA, Liao HX, Tomaras G, Ferrari G, Korber BT, Haynes BF. 2017. Pentavalent HIV-1 vaccine protects against simian-human immunodeficiency virus challenge. Nat Commun 8:15711.
88. Meyerhoff RR, Scearce RM, Ogburn DF, Lockwood B, Pickeral J, Kuraoka M, Anasti K, Eudailey J, Eaton A, Cooper M, Wiehe K, Montefiori DC, Tomaras G, Ferrari G, Alam

bioRxiv preprint doi: https://doi.org/10.1101/2021.11.03.467116; this version posted November 8, 2021. The copyright holder for this preprint (which was not certified by peer review) is the author/funder. All rights reserved. No reuse allowed without permission.

SM, Liao HX, Korber B, Gao F, Haynes BF. 2017. HIV-1 Consensus Envelope-Induced Broadly Binding Antibodies. AIDS Res Hum Retroviruses 33:859-868.

89. Sung JA, Pickeral J, Liu L, Stanfield-Oakley SA, Lam CK, Garrido C, Pollara J, LaBranche C, Bonsignori M, Moody MA, Yang Y, Parks R, Archin N, Allard B, Kirchherr J, Kuruc JD, Gay CL, Cohen MS, Ochsenbauer C, Soderberg K, Liao HX, Montefiori D, Moore P, Johnson S, Koenig S, Haynes BF, Nordstrom JL, Margolis DM, Ferrari G. 2015. Dual-Affinity Re-Targeting proteins direct T cell-mediated cytolysis of latently HIV-infected cells. J Clin Invest doi:10.1172/JCI82314.
90. Tuyishime M, Garrido C, Jha S, Moeser M, Mielke D, LaBranche C, Montefiori D, Haynes BF, Joseph S, Margolis DM, Ferrari G. 2020. Improved killing of HIV-infected cells using three neutralizing and non-neutralizing antibodies. J Clin Invest 130:5157-5170.
91. Bonsignori M, Pollara J, Moody MA, Alpert MD, Chen X, Hwang KK, Gilbert PB, Huang Y, Gurley TC, Kozink DM, Marshall DJ, Whitesides JF, Tsao CY, Kaewkungwal J, Nitayaphan S, Pitisuttithum P, Rerks-Ngarm S, Kim JH, Michael NL, Tomaras GD, Montefiori DC, Lewis GK, Devico A, Evans DT, Ferrari G, Liao HX, Haynes BF. 2012. Antibody-Dependent Cellular Cytotoxicity-Mediating Antibodies from an HIV-1 Vaccine Efficacy Trial Target Multiple Epitopes and Preferentially Use the VH1 Gene Family. J Virol 86:11521-32.
92. Cheng HD, Dowell KG, Bailey-Kellogg C, Goods BA, Love JC, Ferrari G, Alter G, Gach J, Forthal DN, Lewis GK, Greene K, Gao H, Montefiori DC, Ackerman ME. 2021. Diverse antiviral IgG effector activities are predicted by unique biophysical antibody features. Retrovirology 18:35.
93. Pollara J, Jones DI, Huffman T, Edwards RW, Dennis M, Li SH, Jha S, Goodman D, Kumar A, LaBranche CC, Montefiori DC, Fouda GG, Hope TJ, Tomaras GD, Staats HF, Ferrari G, Permar SR. 2019. Bridging Vaccine-Induced HIV-1 Neutralizing and Effector Antibody Responses in Rabbit and Rhesus Macaque Animal Models. J Virol 93.
94. Fisher L, Zinter M, Stanfield-Oakley S, Carpp LN, Edwards RW, Denny T, Moodie Z, Laher F, Bekker LG, McElrath MJ, Gilbert PB, Corey L, Tomaras G, Pollara J, Ferrari G. 2019. Vaccine-Induced Antibodies Mediate Higher Antibody-Dependent Cellular Cytotoxicity After Interleukin-15 Pretreatment of Natural Killer Effector Cells. Front Immunol 10:2741.
95. Lewis GK, Ackerman ME, Scarlatti G, Moog C, Robert-Guroff M, Kent SJ, Overbaugh J, Reeves RK, Ferrari G, Thyagarajan B. 2019. Knowns and Unknowns of Assaying Antibody-Dependent Cell-Mediated Cytotoxicity Against HIV-1. Front Immunol 10:1025.
96. Easterhoff D, Pollara J, Luo K, Tolbert WD, Young B, Mielke D, Jha S, O'Connell RJ, Vasan S, Kim J, Michael NL, Excler JL, Robb ML, Rerks-Ngarm S, Kaewkungwal J, Pitisuttithum P, Nitayaphan S, Sinangil F, Tartaglia J, Phogat S, Kepler TB, Alam SM, Wiehe K, Saunders KO, Montefiori DC, Tomaras GD, Moody MA, Pazgier M, Haynes BF, Ferrari G. 2020. Boosting with AIDSVAX B/E Enhances Env Constant Region 1 and 2 Antibody-Dependent Cellular Cytotoxicity Breadth and Potency. J Virol 94.
97. Tolbert WD, Van V, Sherburn R, Tuyishime M, Yan F, Nguyen DN, Stanfield-Oakley S, Easterhoff D, Bonsignori M, Haynes BF, Moody MA, Ray K, Ferrari G, Lewis GK, Pazgier M. 2020. Recognition Patterns of the C1/C2 Epitopes Involved in Fc-Mediated Response in HIV-1 Natural Infection and the RV114 Vaccine Trial. mBio 11.
98. Madani N, Princiotto AM, Mach L, Ding S, Prevost J, Richard J, Hora B, Sutherland L, Zhao CA, Conn BP, Bradley T, Moody MA, Melillo B, Finzi A, Haynes BF, Smith AB, III, Santra S, Sodroski J. 2018. A CD4-mimetic compound enhances vaccine efficacy against stringent immunodeficiency virus challenge. Nat Commun 9:2363.
99. Strebel K. 2013. HIV accessory proteins versus host restriction factors. Curr Opin Virol 3:692-9.

bioRxiv preprint doi: https://doi.org/10.1101/2021.11.03.467116; this version posted November 8, 2021. The copyright holder for this preprint (which was not certified by peer review) is the author/funder. All rights reserved. No reuse allowed without permission.

100. Ramirez PW, Famiglietti M, Sowrirajan B, DePaula-Silva AB, Rodesch C, Barker E, Bosque A, Planelles V. 2014. Downmodulation of CCR7 by HIV-1 Vpu results in impaired migration and chemotactic signaling within CD4(+) T cells. Cell Rep 7:2019-30.
101. Usami Y, Wu Y, Gottlinger HG. 2015. SERINC3 and SERINC5 restrict HIV-1 infectivity and are counteracted by Nef. Nature 526:218-23.
102. Rosa A, Chande A, Ziglio S, De Sanctis V, Bertorelli R, Goh SL, McCauley SM, Nowosielska A, Antonarakis SE, Luban J, Santoni FA, Pizzato M. 2015. HIV-1 Nef promotes infection by excluding SERINC5 from virion incorporation. Nature 526:212-7.
103. Liu Y, Fu Y, Wang Q, Li M, Zhou Z, Dabbagh D, Fu C, Zhang H, Li S, Zhang T, Gong J, Kong X, Zhai W, Su J, Sun J, Zhang Y, Yu XF, Shao Z, Zhou F, Wu Y, Tan X. 2019. Proteomic profiling of HIV-1 infection of human CD4(+) T cells identifies PSGL-1 as an HIV restriction factor. Nat Microbiol 4:813-825.
104. Fu Y, He S, Waheed AA, Dabbagh D, Zhou Z, Trinite B, Wang Z, Yu J, Wang D, Li F, Levy DN, Shang H, Freed EO, Wu Y. 2020. PSGL-1 restricts HIV-1 infectivity by blocking virus particle attachment to target cells. Proc Natl Acad Sci U S A 117:9537-9545.
105. Schwartz O, Marechal V, Le Gall S, Lemonnier F, Heard JM. 1996. Endocytosis of major histocompatibility complex class I molecules is induced by the HIV-1 Nef protein. Nat Med 2:338-42.
106. Collins KL, Chen BK, Kalams SA, Walker BD, Baltimore D. 1998. HIV-1 Nef protein protects infected primary cells against killing by cytotoxic T lymphocytes. Nature 391:397-401.
107. Cerboni C, Neri F, Casartelli N, Zingoni A, Cosman D, Rossi P, Santoni A, Doria M. 2007. Human immunodeficiency virus 1 Nef protein downmodulates the ligands of the activating receptor NKG2D and inhibits natural killer cell-mediated cytotoxicity. J Gen Virol 88:242-50.
108. Fausther-Bovendo H, Sol-Foulon N, Candotti D, Agut H, Schwartz O, Debre P, Vieillard V. 2009. HIV escape from natural killer cytotoxicity: nef inhibits NKp44L expression on CD4+ T cells. AIDS 23:1077-87.
109. Shah AH, Sowrirajan B, Davis ZB, Ward JP, Campbell EM, Planelles V, Barker E. 2010. Degranulation of natural killer cells following interaction with HIV-1-infected cells is hindered by downmodulation of NTB-A by Vpu. Cell Host Microbe 8:397-409.
110. Matusali G, Potesta M, Santoni A, Cerboni C, Doria M. 2012. The human immunodeficiency virus type 1 Nef and Vpu proteins downregulate the natural killer cell-activating ligand PVR. J Virol 86:4496-504.
111. Apps R, Del Prete GQ, Chatterjee P, Lara A, Brumme ZL, Brockman MA, Neil S, Pickering S, Schneider DK, Piechocka-Trocha A, Walker BD, Thomas R, Shaw GM, Hahn BH, Keele BF, Lifson JD, Carrington M. 2016. HIV-1 Vpu Mediates HLA-C Downregulation. Cell Host Microbe 19:686-95.
112. Moll M, Andersson SK, Smed-Sorensen A, Sandberg JK. 2010. Inhibition of lipid antigen presentation in dendritic cells by HIV-1 Vpu interference with CD1d recycling from endosomal compartments. Blood 116:1876-84.
113. Chen N, McCarthy C, Drakesmith H, Li D, Cerundolo V, McMichael AJ, Screaton GR, Xu XN. 2006. HIV-1 down-regulates the expression of CD1d via Nef. Eur J Immunol 36:278-86.
114. Pacyniak E, Gomez ML, Gomez LM, Mulcahy ER, Jackson M, Hout DR, Wisdom BJ, Stephens EB. 2005. Identification of a region within the cytoplasmic domain of the subtype B Vpu protein of human immunodeficiency virus type 1 (HIV-1) that is responsible for retention in the golgi complex and its absence in the Vpu protein from a subtype C HIV-1. AIDS Res Hum Retroviruses 21:379-94.

bioRxiv preprint doi: https://doi.org/10.1101/2021.11.03.467116; this version posted November 8, 2021. The copyright holder for this preprint (which was not certified by peer review) is the author/funder. All rights reserved. No reuse allowed without permission.

115. Sharma S, Jafari M, Bangar A, William K, Guatelli J, Lewinski MK. 2019. The C-Terminal End of HIV-1 Vpu Has a Clade-Specific Determinant That Antagonizes BST-2 and Facilitates Virion Release. J Virol 93.
116. Pickering S, Hue S, Kim EY, Reddy S, Wolinsky SM, Neil SJ. 2014. Preservation of Tetherin and CD4 Counter-Activities in Circulating Vpu Alleles despite Extensive Sequence Variation within HIV-1 Infected Individuals. PLoS Pathog 10:e1003895.
117. Iwami S, Sato K, Morita S, Inaba H, Kobayashi T, Takeuchi JS, Kimura Y, Misawa N, Ren F, Iwasa Y, Aihara K, Koyanagi Y. 2015. Pandemic HIV-1 Vpu overcomes intrinsic herd immunity mediated by tetherin. Sci Rep 5:12256.
118. Chen BK, Gandhi RT, Baltimore D. 1996. CD4 down-modulation during infection of human T cells with human immunodeficiency virus type 1 involves independent activities of vpu, env, and nef. J Virol 70:6044-53.
119. Richard J, Veillette M, Brassard N, Iyer SS, Roger M, Martin L, Pazgier M, Schon A, Freire E, Routy JP, Smith AB, III, Park J, Jones DM, Courter JR, Melillo BN, Kaufmann DE, Hahn BH, Permar SR, Haynes BF, Madani N, Sodroski JG, Finzi A. 2015. CD4 mimetics sensitize HIV-1-infected cells to ADCC. Proc Natl Acad Sci U S A 112:E2687-94.
120. Prevost J, Zoubchenok D, Richard J, Veillette M, Pacheco B, Coutu M, Brassard N, Parsons MS, Ruxrungtham K, Bunupuradah T, Tovanabutra S, Hwang KK, Moody MA, Haynes BF, Bonsignori M, Sodroski J, Kaufmann DE, Shaw GM, Chenine AL, Finzi A. 2017. Influence of the Envelope gp120 Phe 43 Cavity on HIV-1 Sensitivity to Antibody-Dependent Cell-Mediated Cytotoxicity Responses. J Virol 91.
121. Prevost J, Richard J, Ding S, Pacheco B, Charlebois R, Hahn BH, Kaufmann DE, Finzi A. 2018. Envelope glycoproteins sampling states 2/3 are susceptible to ADCC by sera from HIV-1-infected individuals. Virology 515:38-45.
122. Richard J, Prevost J, von Bredow B, Ding S, Brassard N, Medjahed H, Coutu M, Melillo B, Bibollet-Ruche F, Hahn BH, Kaufmann DE, Smith AB, 3rd, Sodroski J, Sauter D, Kirchhoff F, Gee K, Neil SJ, Evans DT, Finzi A. 2017. BST-2 Expression Modulates Small CD4-Mimetic Sensitization of HIV-1-Infected Cells to Antibody-Dependent Cellular Cytotoxicity. J Virol 91.
123. Mielke D, Stanfield-Oakley S, Borate B, Fisher LH, Faircloth K, Tuyishime M, Greene K, Gao H, Williamson C, Morris L, Ochsenbauer C, Tomaras G, Haynes BF, Montefiori D, Pollara J, deCamp AC, Ferrari G. 2021. Selection of HIV Envelope strains for standardized assessments of vaccine-elicited antibody-dependent cellular cytotoxicity (ADCC)-mediating antibodies. J Virol doi:10.1128/JVI.01643-21:JVI0164321.
124. Prevost J, Tolbert WD, Medjahed H, Sherburn RT, Madani N, Zoubchenok D, Gendron-Lepage G, Gaffney AE, Grenier MC, Kirk S, Vergara N, Han C, Mann BT, Chenine AL, Ahmed A, Chaiken I, Kirchhoff F, Hahn BH, Haim H, Abrams CF, Smith AB, III, Sodroski J, Pazgier M, Finzi A. 2020. The HIV-1 Env gp120 Inner Domain Shapes the Phe43 Cavity and the CD4 Binding Site. mBio 11.
125. Richard J, Prevost J, Alsahafi N, Ding S, Finzi A. 2018. Impact of HIV-1 Envelope Conformation on ADCC Responses. Trends Microbiol 26:253-265.
126. Alpert MD, Heyer LN, Williams DE, Harvey JD, Greenough T, Allhorn M, Evans DT. 2012. A novel assay for antibody-dependent cell-mediated cytotoxicity against HIV-1- or SIV-infected cells reveals incomplete overlap with antibodies measured by neutralization and binding assays. J Virol 86:12039-52.
127. Fontaine J, Chagnon-Choquet J, Valcke HS, Poudrier J, Roger M. 2011. High expression levels of B lymphocyte stimulator (BLyS) by dendritic cells correlate with HIV-related B-cell disease progression in humans. Blood 117:145-55.

bioRxiv preprint doi: https://doi.org/10.1101/2021.11.03.467116; this version posted November 8, 2021. The copyright holder for this preprint (which was not certified by peer review) is the author/funder. All rights reserved. No reuse allowed without permission.

128. Fontaine J, Coutlee F, Tremblay C, Routy JP, Poudrier J, Roger M. 2009. HIV infection affects blood myeloid dendritic cells after successful therapy and despite nonprogressing clinical disease. J Infect Dis 199:1007-18.
129. International HIVCS, Pereyra F, Jia X, McLaren PJ, Telenti A, de Bakker PI, Walker BD, Ripke S, Brumme CJ, Pulit SL, Carrington M, Kadie CM, Carlson JM, Heckerman D, Graham RR, Plenge RM, Deeks SG, Gianniny L, Crawford G, Sullivan J, Gonzalez E, Davies L, Camargo A, Moore JM, Beattie N, Gupta S, Crenshaw A, Burtt NP, Guiducci C, Gupta N, Gao X, Qi Y, Yuki Y, Piechocka-Trocha A, Cutrell E, Rosenberg R, Moss KL, Lemay P, O'Leary J, Schaefer T, Verma P, Toth I, Block B, Baker B, Rothchild A, Lian J, Proudfoot J, Alvino DM, Vine S, Addo MM, et al. 2010. The major genetic determinants of HIV-1 control affect HLA class I peptide presentation. Science 330:1551-7.
130. Kamya P, Boulet S, Tsoukas CM, Routy JP, Thomas R, Cote P, Boulassel MR, Baril JG, Kovacs C, Migueles SA, Connors M, Suscovich TJ, Brander C, Tremblay CL, Bernard N. 2011. Receptor-ligand requirements for increased NK cell polyfunctional potential in slow progressors infected with HIV-1 coexpressing KIR3DL1*h/*y and HLA-B*57. J Virol 85:5949-60.
131. Peretz Y, Ndongala ML, Boulet S, Boulassel MR, Rouleau D, Cote P, Longpre D, Routy JP, Falutz J, Tremblay C, Tsoukas CM, Sekaly RP, Bernard NF. 2007. Functional T cell subsets contribute differentially to HIV peptide-specific responses within infected individuals: correlation of these functional T cell subsets with markers of disease progression. Clin Immunol 124:57-68.
132. Finzi A, Xiang SH, Pacheco B, Wang L, Haight J, Kassa A, Danek B, Pancera M, Kwong PD, Sodroski J. 2010. Topological layers in the HIV-1 gp120 inner domain regulate gp41 interaction and CD4-triggered conformational transitions. Mol Cell 37:656-67.
133. Emi N, Friedmann T, Yee JK. 1991. Pseudotype formation of murine leukemia virus with the G protein of vesicular stomatitis virus. J Virol 65:1202-7.
134. Salazar-Gonzalez JF, Salazar MG, Keele BF, Learn GH, Giorgi EE, Li H, Decker JM, Wang S, Baalwa J, Kraus MH, Parrish NF, Shaw KS, Guffey MB, Bar KJ, Davis KL, Ochsenbauer-Jambor C, Kappes JC, Saag MS, Cohen MS, Mulenga J, Derdeyn CA, Allen S, Hunter E, Markowitz M, Hraber P, Perelson AS, Bhattacharya T, Haynes BF, Korber BT, Hahn BH, Shaw GM. 2009. Genetic identity, biological phenotype, and evolutionary pathways of transmitted/founder viruses in acute and early HIV-1 infection. J Exp Med 206:1273-89.
135. Ochsenbauer C, Edmonds TG, Ding H, Keele BF, Decker J, Salazar MG, Salazar-Gonzalez JF, Shattock R, Haynes BF, Shaw GM, Hahn BH, Kappes JC. 2012. Generation of Transmitted/Founder HIV-1 Infectious Molecular Clones and Characterization of Their Replication Capacity in CD4 T Lymphocytes and Monocyte-Derived Macrophages. J Virol 86:2715-28.
136. Parrish NF, Wilen CB, Banks LB, Iyer SS, Pfaff JM, Salazar-Gonzalez JF, Salazar MG, Decker JM, Parrish EH, Berg A, Hopper J, Hora B, Kumar A, Mahlokozera T, Yuan S, Coleman C, Vermeulen M, Ding H, Ochsenbauer C, Tilton JC, Permar SR, Kappes JC, Betts MR, Busch MP, Gao F, Montefiori D, Haynes BF, Shaw GM, Hahn BH, Doms RW. 2012. Transmitted/founder and chronic subtype C HIV-1 use CD4 and CCR5 receptors with equal efficiency and are not inhibited by blocking the integrin alpha4beta7. PLoS Pathog 8:e1002686.
137. Parrish NF, Gao F, Li H, Giorgi EE, Barbian HJ, Parrish EH, Zajic L, Iyer SS, Decker JM, Kumar A, Hora B, Berg A, Cai F, Hopper J, Denny TN, Ding H, Ochsenbauer C, Kappes JC, Galimidi RP, West AP, Jr., Bjorkman PJ, Wilen CB, Doms RW, O'Brien M, Bhardwaj N, Borrow P, Haynes BF, Muldoon M, Theiler JP, Korber B, Shaw GM, Hahn BH. 2013.

bioRxiv preprint doi: https://doi.org/10.1101/2021.11.03.467116; this version posted November 8, 2021. The copyright holder for this preprint (which was not certified by peer review) is the author/funder. All rights reserved. No reuse allowed without permission.

Phenotypic properties of transmitted founder HIV-1. Proc Natl Acad Sci U S A 110:6626-33.

138. Fenton-May AE, Dibben O, Emmerich T, Ding H, Pfafferott K, Aasa-Chapman MM, Pellegrino P, Williams I, Cohen MS, Gao F, Shaw GM, Hahn BH, Ochsenbauer C, Kappes JC, Borrow P. 2013. Relative resistance of HIV-1 founder viruses to control by interferon-alpha. Retrovirology 10:146.
139. Liao HX, Lynch R, Zhou T, Gao F, Alam SM, Boyd SD, Fire AZ, Roskin KM, Schramm CA, Zhang Z, Zhu J, Shapiro L, Mullikin JC, Gnanakaran S, Hraber P, Wiehe K, Kelsoe G, Yang G, Xia SM, Montefiori DC, Parks R, Lloyd KE, Scearce RM, Soderberg KA, Cohen M, Kamanga G, Louder MK, Tran LM, Chen Y, Cai F, Chen S, Moquin S, Du X, Joyce MG, Srivatsan S, Zhang B, Zheng A, Shaw GM, Hahn BH, Kepler TB, Korber BT, Kwong PD, Mascola JR, Haynes BF. 2013. Co-evolution of a broadly neutralizing HIV-1 antibody and founder virus. Nature 496:469-76.
140. Gao F, Bonsignori M, Liao HX, Kumar A, Xia SM, Lu X, Cai F, Hwang KK, Song H, Zhou T, Lynch RM, Alam SM, Moody MA, Ferrari G, Berrong M, Kelsoe G, Shaw GM, Hahn BH, Montefiori DC, Kamanga G, Cohen MS, Hraber P, Kwong PD, Korber BT, Mascola JR, Kepler TB, Haynes BF. 2014. Cooperation of B cell lineages in induction of HIV-1-broadly neutralizing antibodies. Cell 158:481-91.
141. Salminen MO, Ehrenberg PK, Mascola JR, Dayhoff DE, Merling R, Blake B, Louder M, Hegerich S, Polonis VR, Birx DL, Robb ML, McCutchan FE, Michael NL. 2000. Construction and biological characterization of infectious molecular clones of HIV-1 subtypes B and E (CRF01_AE) generated by the polymerase chain reaction. Virology 278:103-10.
142. Chenine AL, Merbah M, Wieczorek L, Molnar S, Mann B, Lee J, O'Sullivan AM, Bose M, Sanders-Buell E, Kijak GH, Herrera C, McLinden R, O'Connell RJ, Michael NL, Robb ML, Kim JH, Polonis VR, Tovanabutra S. 2018. Neutralization Sensitivity of a Novel HIV-1 CRF01_AE Panel of Infectious Molecular Clones. J Acquir Immune Defic Syndr 78:348-355.
143. Peachman KK, Karasavvas N, Chenine AL, McLinden R, Rerks-Ngarm S, Jaranit K, Nitayaphan S, Pitisuttithum P, Tovanabutra S, Zolla-Pazner S, Michael NL, Kim JH, Alving CR, Rao M. 2015. Identification of New Regions in HIV-1 gp120 Variable 2 and 3 Loops that Bind to alpha4beta7 Integrin Receptor. PLoS One 10:e0143895.
144. O'Brien WA, Koyanagi Y, Namazie A, Zhao JQ, Diagne A, Idler K, Zack JA, Chen IS. 1990. HIV-1 tropism for mononuclear phagocytes can be determined by regions of gp120 outside the CD4-binding domain. Nature 348:69-73.
145. Li Y, Kappes JC, Conway JA, Price RW, Shaw GM, Hahn BH. 1991. Molecular characterization of human immunodeficiency virus type 1 cloned directly from uncultured human brain tissue: identification of replication-competent and -defective viral genomes. J Virol 65:3973-85.
146. Theodore TS, Englund G, Buckler-White A, Buckler CE, Martin MA, Peden KW. 1996. Construction and characterization of a stable full-length macrophage-tropic HIV type 1 molecular clone that directs the production of high titers of progeny virions. AIDS Res Hum Retroviruses 12:191-4.
147. Krapp C, Hotter D, Gawanbacht A, McLaren PJ, Kluge SF, Sturzel CM, Mack K, Reith E, Engelhart S, Ciuffi A, Hornung V, Sauter D, Telenti A, Kirchhoff F. 2016. Guanylate Binding Protein (GBP) 5 Is an Interferon-Inducible Inhibitor of HIV-1 Infectivity. Cell Host Microbe 19:504-14.
148. Koyanagi Y, Miles S, Mitsuyasu RT, Merrill JE, Vinters HV, Chen IS. 1987. Dual infection of the central nervous system by AIDS viruses with distinct cellular tropisms. Science 236:819-22.

bioRxiv preprint doi: https://doi.org/10.1101/2021.11.03.467116; this version posted November 8, 2021. The copyright holder for this preprint (which was not certified by peer review) is the author/funder. All rights reserved. No reuse allowed without permission.

149. Adachi A, Gendelman HE, Koenig S, Folks T, Willey R, Rabson A, Martin MA. 1986. Production of acquired immunodeficiency syndrome-associated retrovirus in human and nonhuman cells transfected with an infectious molecular clone. J Virol 59:284-91.
150. Mack K, Starz K, Sauter D, Langer S, Bibollet-Ruche F, Learn GH, Sturzel CM, Leoz M, Plantier JC, Geyer M, Hahn BH, Kirchhoff F. 2017. Efficient Vpu-Mediated Tetherin Antagonism by an HIV-1 Group O Strain. J Virol 91.
151. Takehisa J, Kraus MH, Decker JM, Li Y, Keele BF, Bibollet-Ruche F, Zammit KP, Weng Z, Santiago ML, Kamenya S, Wilson ML, Pusey AE, Bailes E, Sharp PM, Shaw GM, Hahn BH. 2007. Generation of infectious molecular clones of simian immunodeficiency virus from fecal consensus sequences of wild chimpanzees. J Virol 81:7463-75.
152. Shingai M, Donau OK, Schmidt SD, Gautam R, Plishka RJ, Buckler-White A, Sadjadpour R, Lee WR, LaBranche CC, Montefiori DC, Mascola JR, Nishimura Y, Martin MA. 2012. Most rhesus macaques infected with the CCR5-tropic SHIV(AD8) generate cross-reactive antibodies that neutralize multiple HIV-1 strains. Proc Natl Acad Sci U S A 109:19769-74.
153. Li H, Wang S, Lee FH, Roark RS, Murphy AI, Smith J, Zhao C, Rando J, Chohan N, Ding Y, Kim E, Lindemuth E, Bar KJ, Pandrea I, Apetrei C, Keele BF, Lifson JD, Lewis MG, Denny TN, Haynes BF, Hahn BH, Shaw GM. 2021. New SHIVs and Improved Design Strategy for Modeling HIV-1 Transmission, Immunopathogenesis, Prevention and Cure. J Virol doi:10.1128/JVI.00071-21.
154. R Core Team. 2013. R: A language and environment for statistical computing, R Foundation for Statistical Computing, Vienna, Austria. https://www.R-project.org/.
155. RStudio team. 2015. RStudio: Integrated Development for R, RStudio, Inc., Boston, MA. http://www.rstudio.com/.

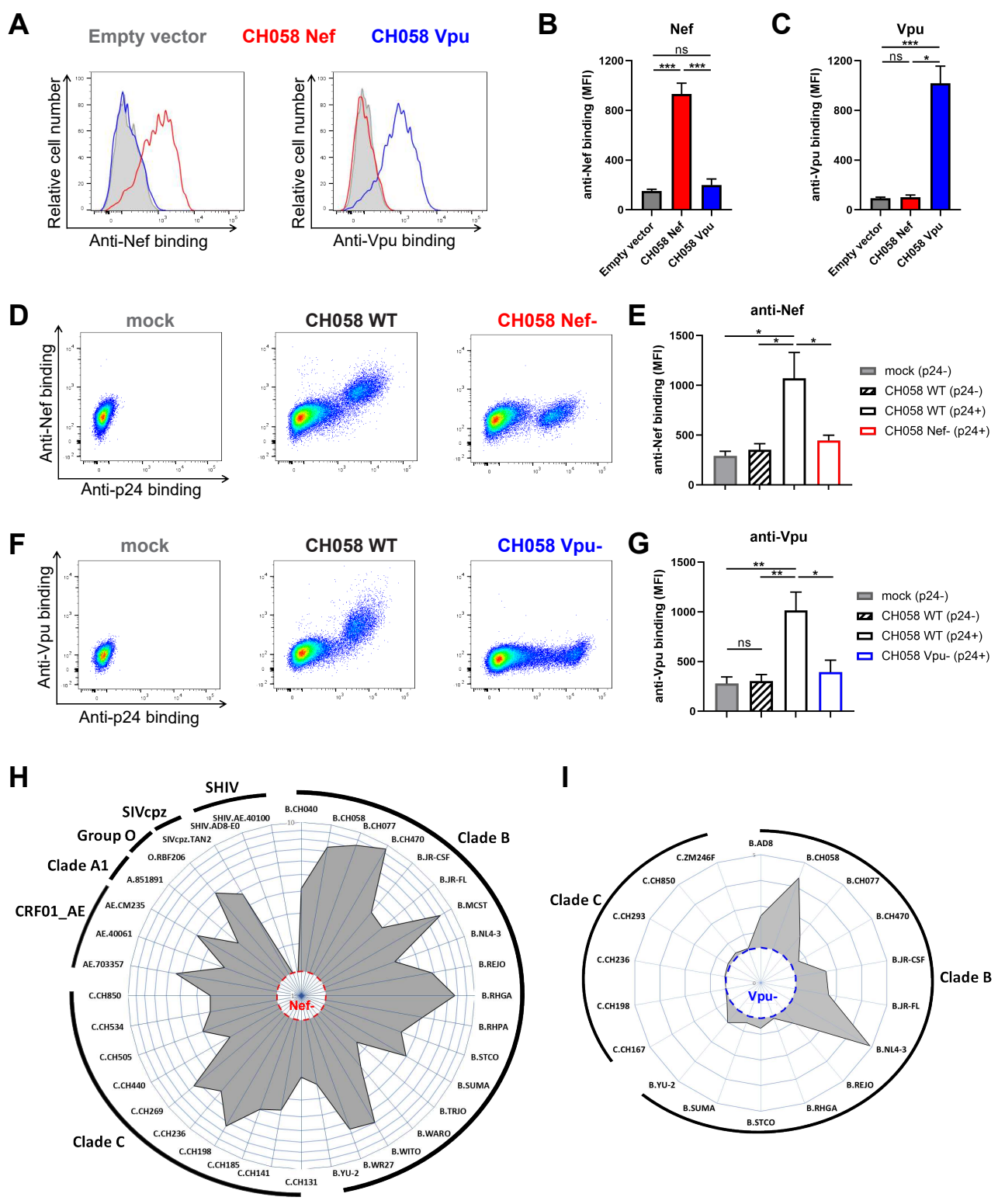
A
Empty vector
CH058 Nef
CH058 Vpu
Relative cell number
Anti-Nef binding
Relative cell number
Anti-Vpu binding
B
Nef
anti-Nef binding (MFI)
ns
***
***
1200
800
400
0
Empty vector
CH058 Nef
CH058 Vpu
C
Vpu
anti-Vpu binding (MFI)
***
ns
*
1200
800
400
0
Empty vector
CH058 Nef
CH058 Vpu
D
mock
CH058 WT
CH058 Nef-
Anti-Nef binding
Anti-p24 binding
E
anti-Nef
anti-Nef binding (MFI)
1500
1000
500
0
mock (p24-)
CH058 WT (p24-)
CH058 WT (p24+)
CH058 Nef- (p24+)
F
mock
CH058 WT
CH058 Vpu-
Anti-Vpu binding
Anti-p24 binding
G
anti-Vpu
anti-Vpu binding (MFI)
1500
1000
500
0
ns
mock (p24-)
CH058 WT (p24-)
CH058 WT (p24+)
CH058 Vpu- (p24+)
H
SHIV
SIVcpz
Group O
Clade A1
CRF01_AE
Clade C
Clade B
SHIV.AE.40100
SHIV.AD8-E0
SIVcpz.TAN2
O.RBF206
A.851891
AE.CM235
AE.40061
AE.703357
C.CH850
C.CH534
C.CH505
C.CH440
C.CH269
C.CH236
C.CH198
C.CH185
C.CH141
C.CH131
B.YU-2
B.WR27
B.WITO
B.WARO
B.TRJO
B.SUMA
B.STCO
B.RHPA
B.RHGA
B.REJO
B.NL4-3
B.MCST
B.JR-FL
B.JR-CSF
B.CH470
B.CH077
B.CH058
B.CH040
Nef-
I
Clade C
Clade B
B.AD8
B.CH058
B.CH077
B.CH470
B.JR-CSF
B.JR-FL
B.NL4-3
B.REJO
B.RHGA
B.STCO
B.SUMA
B.YU-2
C.CH167
C.CH198
C.CH236
C.CH293
C.CH850
C.ZM246F
Vpu-

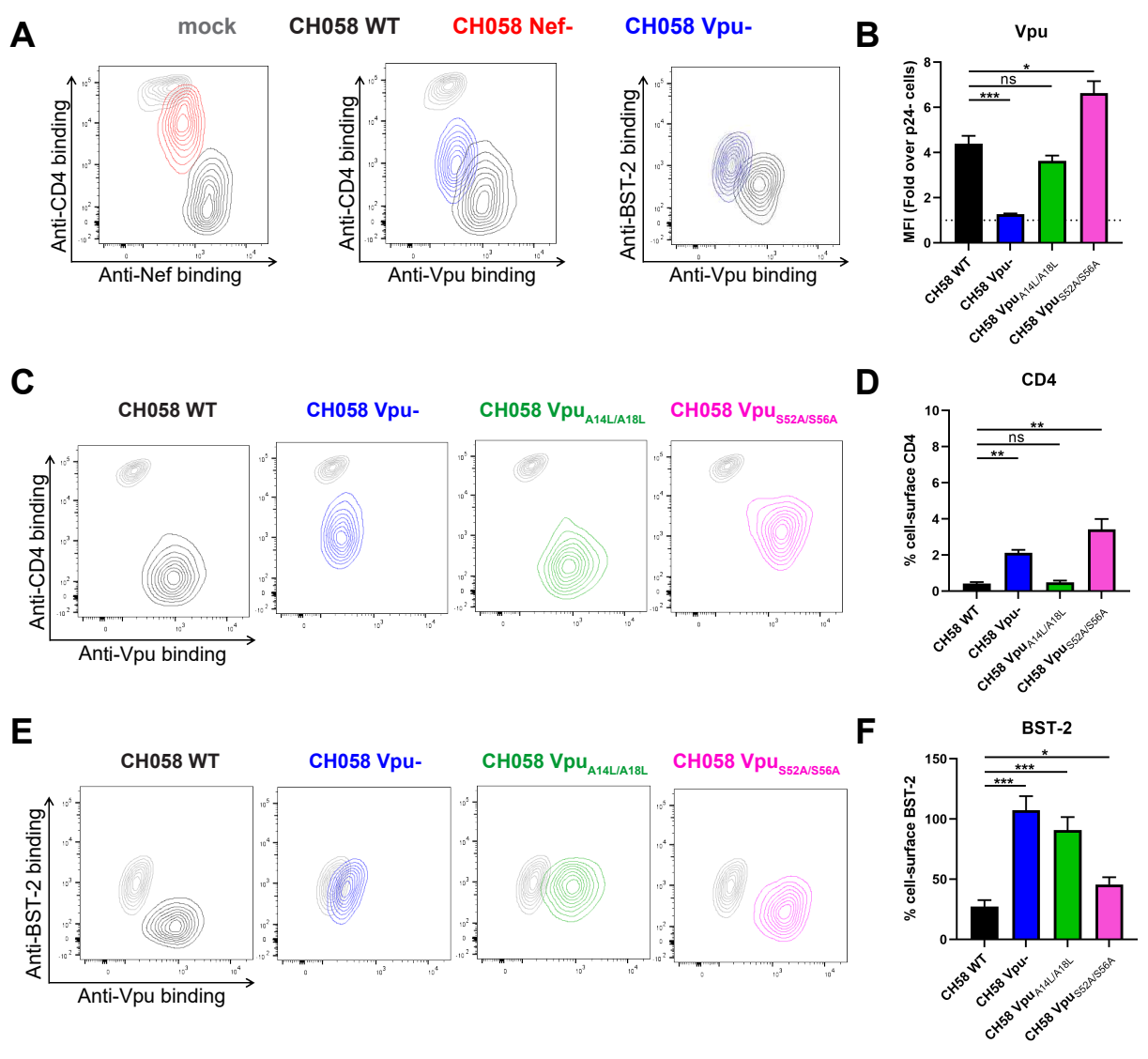
A
mock
CH058 WT
CH058 Nef-
CH058 Vpu-
Anti-CD4 binding
Anti-Nef binding
Anti-CD4 binding
Anti-Vpu binding
Anti-BST-2 binding
Anti-Vpu binding
B
Vpu
MFI (Fold over p24- cells)
ns
*
***
CH58 WT
CH58 Vpu-
CH58 VpuA14L/A18L
CH58 VpuS52A/S56A
C
CH058 WT
CH058 Vpu-
CH058 VpuA14L/A18L
CH058 VpuS52A/S56A
Anti-CD4 binding
Anti-Vpu binding
D
CD4
% cell-surface CD4
**
ns
**
CH58 WT
CH58 Vpu-
CH58 VpuA14L/A18L
CH58 VpuS52A/S56A
E
CH058 WT
CH058 Vpu-
CH058 VpuA14L/A18L
CH058 VpuS52A/S56A
Anti-BST-2 binding
Anti-Vpu binding
F
BST-2
% cell-surface BST-2
*
***
***
CH58 WT
CH58 Vpu-
CH58 VpuA14L/A18L
CH58 VpuS52A/S56A

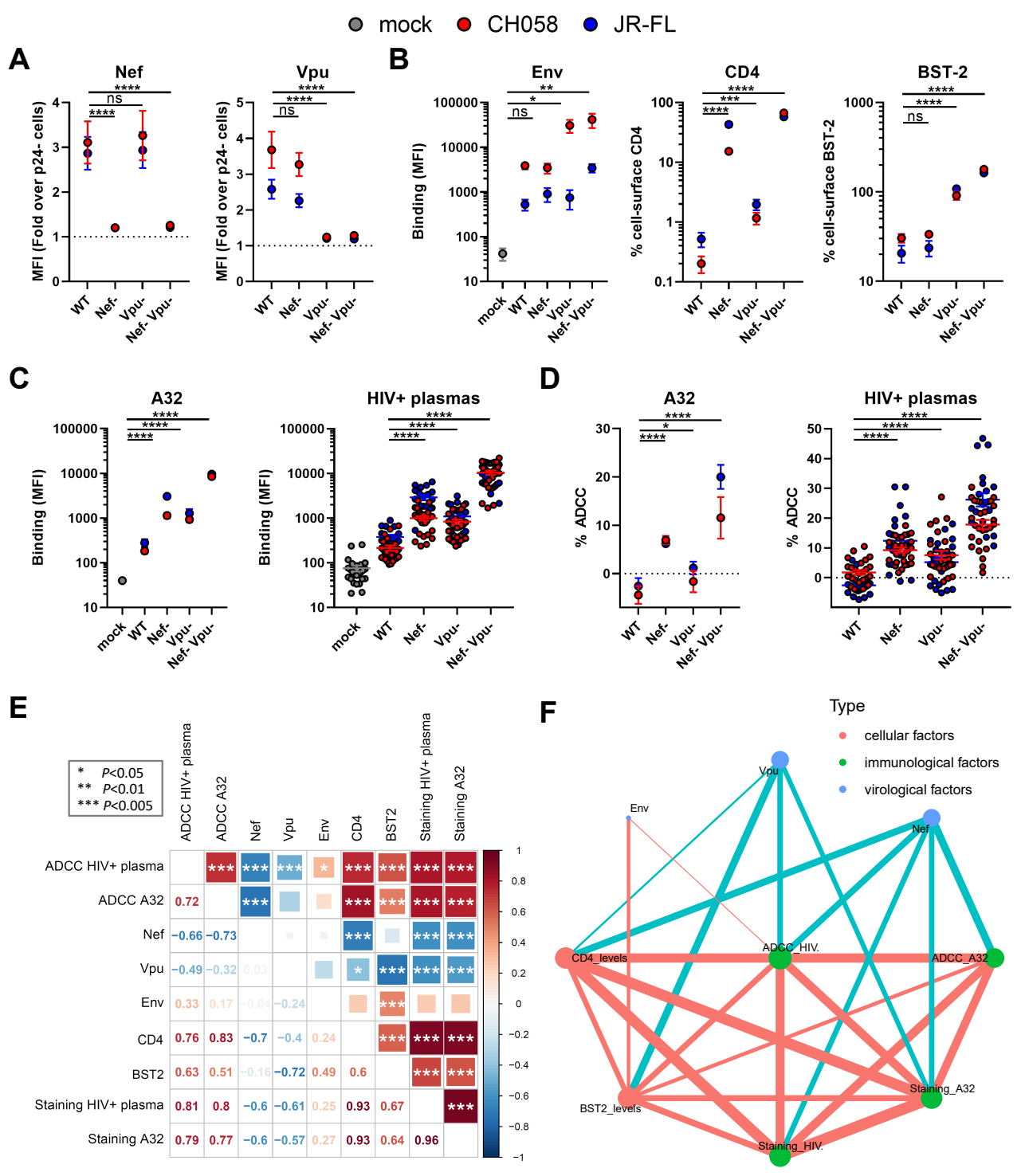
mock
CH058
JR-FL
A
Nef
Vpu
MFI (Fold over p24- cells)
WT
Nef-
Vpu-
Nef- Vpu-
B
Env
CD4
BST-2
Binding (MFI)
% cell-surface CD4
% cell-surface BST-2
C
A32
HIV+ plasmas
D
% ADCC
E
* P<0.05
** P<0.01
*** P<0.005
ADCC HIV+ plasma
ADCC A32
Nef
Vpu
Env
CD4
BST2
Staining HIV+ plasma
Staining A32
F
Type
cellular factors
immunological factors
virological factors
CD4_levels
ADCC_HIV.
ADCC_A32
BST2_levels
Staining_HIV.
Staining_A32

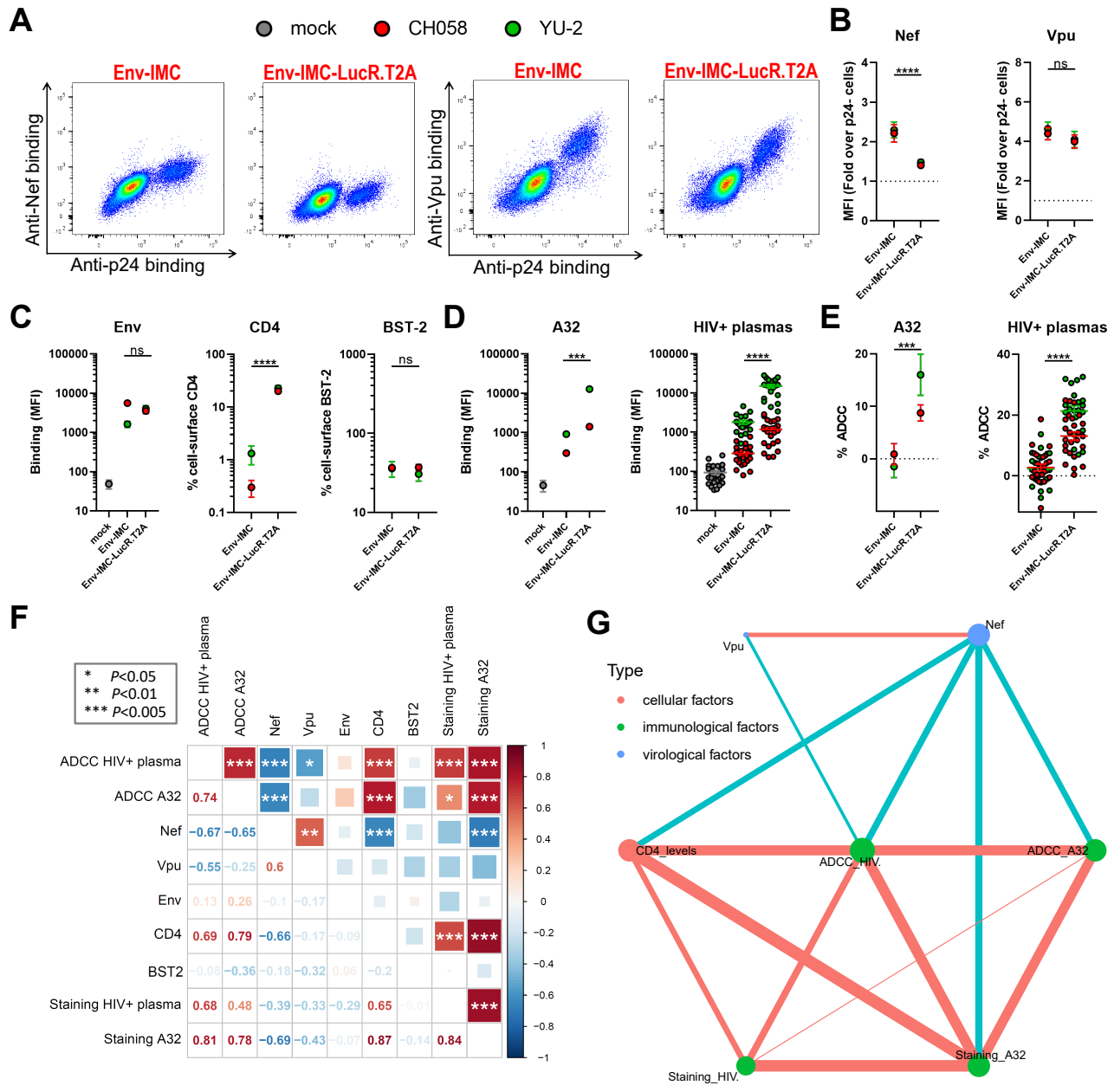
A
mock
CH058
YU-2
Env-IMC
Env-IMC-LucR.T2A
Anti-Nef binding
Anti-p24 binding
Anti-Vpu binding
B
Nef
Vpu
MFI (Fold over p24- cells)
****
ns
C
Env
CD4
BST-2
Binding (MFI)
% cell-surface CD4
% cell-surface BST-2
D
A32
HIV+ plasmas
***
E
% ADCC
F
* P<0.05
** P<0.01
*** P<0.005
ADCC HIV+ plasma
ADCC A32
Nef
Vpu
Env
CD4
BST2
Staining HIV+ plasma
Staining A32
G
Type
cellular factors
immunological factors
virological factors
CD4_levels
ADCC_HIV.
ADCC_A32
Staining_HIV.
Staining_A32

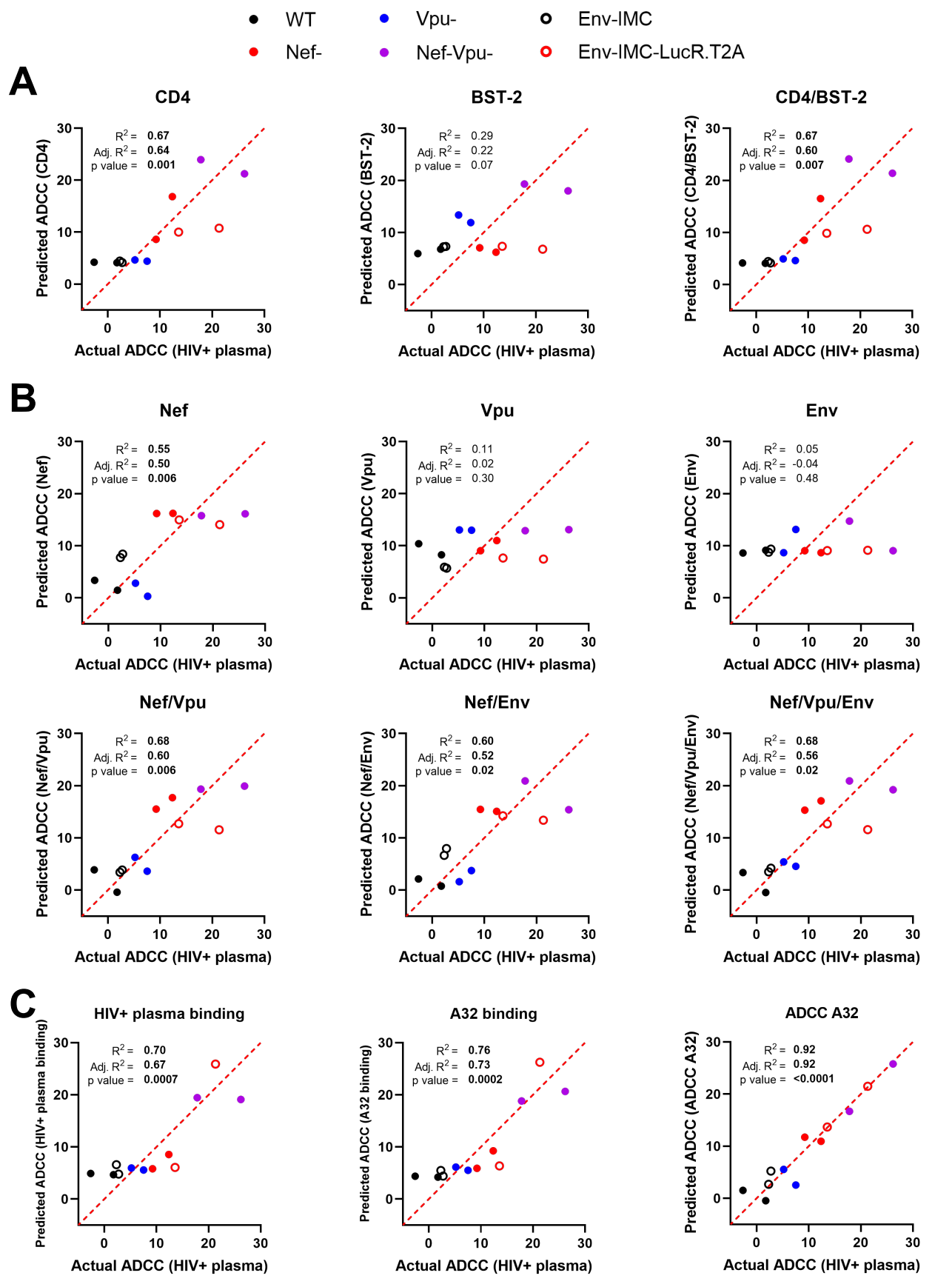
WT
Nef-
Vpu-
Nef-Vpu-
Env-IMC
Env-IMC-LucR.T2A
A
CD4
Predicted ADCC (CD4)
R² = 0.67
Adj. R² = 0.64
p value = 0.001
BST-2
Predicted ADCC (BST-2)
R² = 0.29
Adj. R² = 0.22
p value = 0.07
CD4/BST-2
Predicted ADCC (CD4/BST-2)
R² = 0.67
Adj. R² = 0.60
p value = 0.007
Actual ADCC (HIV+ plasma)
B
Nef
Predicted ADCC (Nef)
R² = 0.55
Adj. R² = 0.50
p value = 0.006
Vpu
Predicted ADCC (Vpu)
R² = 0.11
Adj. R² = 0.02
p value = 0.30
Env
Predicted ADCC (Env)
R² = 0.05
Adj. R² = -0.04
p value = 0.48
Nef/Vpu
Predicted ADCC (Nef/Vpu)
R² = 0.68
Adj. R² = 0.60
p value = 0.006
Nef/Env
Predicted ADCC (Nef/Env)
R² = 0.60
Adj. R² = 0.52
p value = 0.02
Nef/Vpu/Env
Predicted ADCC (Nef/Vpu/Env)
R² = 0.68
Adj. R² = 0.56
p value = 0.02
C
HIV+ plasma binding
Predicted ADCC (HIV+ plasma binding)
R² = 0.70
Adj. R² = 0.67
p value = 0.0007
A32 binding
Predicted ADCC (A32 binding)
R² = 0.76
Adj. R² = 0.73
p value = 0.0002
ADCC A32
Predicted ADCC (ADCC A32)
R² = 0.92
Adj. R² = 0.92
p value = <0.0001